Accepted Manuscript

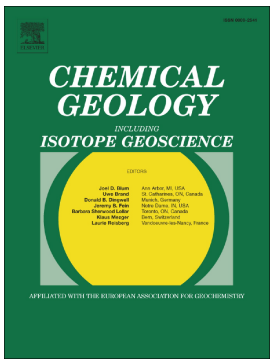

Further evaluation of the Re-Os systematics of crude oil: Implications for Re-Os geochronology of petroleum systems

Junjie Liu, David Selby, Honggang Zhou, Magali Pujol

PII: S0009-2541(19)30102-0
DOI: https://doi.org/10.1016/j.chemgeo.2019.03.004
Reference: CHEMGE 19093

To appear in: *Chemical Geology*

Received date: 26 June 2018
Revised date: 17 December 2018
Accepted date: 4 March 2019

Please cite this article as: J. Liu, D. Selby, H. Zhou, et al., Further evaluation of the Re-Os systematics of crude oil: Implications for Re-Os geochronology of petroleum systems, Chemical Geology, https://doi.org/10.1016/j.chemgeo.2019.03.004

Further evaluation of the Re-Os systematics of crude oil: Implications for Re-Os geochronology of petroleum systems

Junjie Liu[1], David Selby[1&2], Honggang Zhou[3] and Magali Pujol[3]

[1]Deparment of Earth Sciences, Durham University, Durham, DH1 3LE, UK.

[2]State Key Laboratory of Geological Processes and Mineral Resources, School of Earth Resources, China University of Geosciences Wuhan, Wuhan, China.

[3]TOTAL, Centre Scientifique et Techniques Jean-Féger, Pau, France.

Corresponding author: Junjie Liu (junjie.liu@durham.ac.uk)

Keywords:

Re-Os systematics; Crude oil; Progressive precipitation; *N*-alkanes asphaltene separation; Re-Os geochronology.

Abstract

Here we further demonstrate asphaltene to be the main carrier of Re and Os in crude oil and additionally show that generally the less soluble fractions of asphaltene contain higher concentrations of Re and Os, with the $^{187}Os/^{188}Os$ and $^{187}Re/^{188}Os$ values showing different trends between oils. These observations are considered as evidence of the existence of different Re and Os carriers in crude oil. The multiple heteroatomic ligands and porphyrins proposed as Re and Os hosts in crude oil are likely present as free molecules, initially absorbed and occluded in the asphaltene aggregates and co-precipitate with asphaltene in response to the addition of *n*-alkanes. The Re-Os elemental and isotopic systematic behaviour revealed herein are interpreted to be the result of the involvement of Re and Os carriers in the aggregation and precipitation of asphaltene, and the chemical make-up of each particular crude oil.

Asphaltene and maltene separated by a series of different alkanes show that asphaltene yields decrease from *n*-pentane to *n*-heptane and then tend to stay stable until *n*-decane. The $^{187}Os/^{188}Os$ values of the series of asphaltenes are extremely similar for each oil sample, inhibiting the possibility of determining any Re-Os dates with the asphaltenes of a single crude oil. In contrast, the maltene fractions exhibit Re-Os isotopic variation. Nevertheless, only the maltenes of one oil defined a reasonable isochron with an age similar to that of source rock. As such, this study highlights the need for a greater understanding in order to determine whether, and in what cases, fractions separated from a single crude oil by different alkanes can provide meaningful Re-Os ages.

Highlights:

- The Re and Os concentrations of the progressively precipitated asphaltene fractions generally decrease with the increase of *n*-heptane in its mixture with DCM.
- The $^{187}Os/^{188}Os$ and $^{187}Re/^{188}Os$ of the progressively precipitated asphaltene fractions show different trends between oils.
- Single oil separation into fractions using different alkanes may not always be able to yield meaningful chronological data.

1 Introduction

The presence of rhenium (Re) and osmium (Os) in measurable concentrations in many bitumen and crude oil samples, typically > 1 ppb (parts per billion of mass, ng/g) Re and > 30 ppt (parts per trillion of mass, pg/g) Os, has been known for several decades (Poplavko *et al.*, 1974; Barre *et al.*, 1995; Selby *et al.*, 2007). As a result, this has opened the possibility that the Re-Os geochronometer may provide timing constraints for key petroleum events, e.g., crude oil generation, thermochemical sulphate reduction and thermal cracking, and also that Os isotopes ($^{187}Os/^{188}Os$) may serve as source tracers of the oil (Selby *et al.*, 2005; Selby & Creaser, 2005; Finlay *et al.*, 2011; Finlay *et al.*, 2012; Lillis & Selby, 2013; Cumming *et al.*, 2014; Ge *et al.*, 2016; Ge *et al.*, 2017a; Ge *et al.*, 2017b; Liu *et al.*, 2018). Thus far, the validation of Re-Os crude oil and bitumen dates are commonly achieved through the comparison with the established chronologies of the studied petroleum systems, e.g. basin modelling, apatite fission track and Ar-Ar dates. Therefore, it is now critical to enhance the understanding of the elemental and isotopic systematics and the geochemical behaviour of Re and Os in crude oil for the interpretation and further application of Re-Os geochronometer to petroleum systems.

It has been shown that the asphaltene fraction isolated from crude oil by the addition of *n*-alkanes (e.g. *n*-pentane and *n*-heptane) is the main carrier of Re (> 90%) and Os (> 83%) in crude oil (Selby *et al.*, 2007; Rooney *et al.*, 2012; Georgiev *et al.*, 2016; Liu & Selby, 2018). As a result, the Re-Os isotopic systematics (i.e. the $^{187}Re/^{188}Os$ and $^{187}Os/^{188}Os$ values, ratio of the number of atoms) of the whole oil are predominantly determined by the asphaltene fraction (Selby *et al.*, 2007; Liu & Selby, 2018). The exact binding locations of both Re and Os in the asphaltene and maltene fractions still remain mostly unknown, although previous studies have proposed that Re and Os are present in the form of metalloporphyrins or to be bound by heteroatom ligands (Miller, 2004; Selby *et al.*, 2007; Rooney *et al.*, 2012; DiMarzio *et al.*, 2018).

The typical models of the molecular structure of asphaltene consist of a single polycyclic aromatic hydrocarbon core known as the island or continental type (Mullins, 2010), or multiple alkyl-bridged aromatic cores known as the archipelago type (Strausz *et al.*, 1992; Murgich *et al.*, 1999; Chacón-Patiño *et al.*, 2017) with pendant alkyl chains and functional groups. The asphaltene molecules tend to aggregate even at low concentrations (50-100 mg/l) in solvents like toluene (Durand *et al.*, 2010; Mullins *et al.*, 2012; Yarranton *et al.*, 2013), forming structures which could occlude and adsorb surrounding molecules. Asphaltene precipitation occurs in response to the changes in physical and chemical conditions within the petroleum system, e.g., pressure decrease and component changes, including gas (CH_4 and CO_2) injection and oil mixing (Buenrostro-Gonzalez *et al.*, 2004; Subramanian *et al.*, 2016). To date, the studies of Re-Os elemental and isotopic systematics have been conducted on sequentially precipitated fractions from asphaltenes (Mahdaoui *et al.*, 2013; DiMarzio *et al.*, 2018). For the two samples studied by Mahdaoui *et al.* (2013), sequential precipitation of asphaltenes was conducted with a mixture of dichloromethane (CH_2Cl_2, DCM) and *n*-heptane or *n*-pentane. The Re and Os concentrations of the progressively precipitated asphaltene fractions decrease throughout the process, however both the ratios of the Re/Os and $^{187}Os/^{188}Os$ of the fractions remain nearly constant. (DiMarzio *et al.*, 2018) utilized two different mixtures, *n*-heptane-DCM and acetone-

toluene, for the sequential precipitation of two aliquots of the same asphaltene from a heavy oil sample. This study showed that the highest Re and Os concentrations are observed in the intermediate soluble fraction separated by *n*-heptane-DCM, and the most insoluble fraction separated by acetone-toluene with a few exceptions. In contrast to the study of Mahdaoui *et al.* (2013), the $^{187}Re/^{188}Os$ values of the fractions separated by acetone-toluene fluctuate throughout the progressive precipitation, with the corresponding $^{187}Os/^{188}Os$ compositions of the fractions remaining fairly constant throughout. For the fractions separated by *n*-heptane-DCM, $^{187}Re/^{188}Os$ increases, and $^{187}Os/^{188}Os$ increases at first and then decreases throughout the progressive precipitation.

The substitution of the analysis of some low Re and Os bearing crude oils with its more Re-Os enriched asphaltene fraction for better measurement precision and applying a sampling methodology of multiple samples over large distances for Re-Os dating of petroleum systems has been applied (Finlay *et al.*, 2011; Lillis & Selby, 2013; Cumming *et al.*, 2014; Liu *et al.*, 2018). In contrast, a new sampling methodology for Re-Os dating of crude oil was proposed to avoid the potential disadvantages of using multiple crude oil samples from a large geographic area, e.g. different sources, different generation and migration ages, and different secondary/alteration histories (Georgiev *et al.*, 2016). The new sampling methodology was used to conduct Re-Os analyses on multiple asphaltene and maltene fractions separated from a single crude oil sample with *n*-pentane, *n*-hexane, *n*-heptane and *n*-decane with the objective of obtaining a spread in Re-Os isotopic compositions sufficient to develop an isochron. Applied in the Gela oilfield of Italy, the Re-Os dates were defined by the maltene fractions of an oil sample from the Streppenosa Formation (~ 200 Ma) and by the crude oil and asphaltene fractions of another two oils from the Noto and Sciacca Formations (~ 28 Ma). These Re-Os dates are interpreted to reflect the timing of oil generation (Georgiev *et al.*, 2016).

Although the previous studies have greatly increased the knowledge of the Re-Os systematics within crude oil and asphaltene, the current understanding may be limited by the small number of samples employed, the substantial complexity and diversity of worldwide crude oils, and the interpretation of current data. Further, the ability of the single oil Re-Os dating method to determine geological age also requires further examination before extensive application. In this study, the Re-Os elemental and isotopic systematics of six different crude oils were inspected by separating them into two sets of fractions with two different methodologies: 1) fractionating bulk asphaltene progressively with the increase of *n*-heptane percentage in its mixture with DCM, and, 2) separating whole oil into asphaltene and maltene fractions using a series of *n*-alkane solutions (from *n*-C_5 to *n*-C_{10}) with DCM-methanol. This study illustrates the observed decrease of Re and Os concentrations and the different trends in the $^{187}Re/^{188}Os$ and $^{187}Os/^{188}Os$ compositions throughout the progressive precipitation for each of the six samples studied. This study also suggests that the Re-Os elemental and isotopic systematics are closely related to the aggregation and precipitation process of the asphaltene. It is observed that the variation of Re-Os isotopic compositions of the maltene fractions separated by the series of *n*-alkane solutions is more prominent than that of the asphaltene fractions. However, given the data of the six oils studied here, the Re-Os systematics of either the asphaltene or the maltene fractions of a single crude oil cannot consistently yield geologically meaningful dates. This finding does not

support the widespread application of the Re-Os system to obtain chronological information from individual crude oils.

2 Samples and analytical protocols

2.1 The samples

Six crude oils of different geographic origins are used in this study, of which the Derby, Federal, Purisima and Viking-Morel oil samples were obtained from the U.S. Geological Survey (USGS) oil library in Denver, Colorado, the Persian oil was provided by Centre Scientifique et Technique Jean Féger (CSTJF) of the TOTAL petroleum company, the RM8505 was ordered from the U.S. National Institute of Standards and Technology (NIST) and has recently been developed as a reference material for Re-Os hydrocarbon analysis (Liu & Selby, 2018).

The Derby oil (108.55°W, 42.69°N) is recovered from the Permian Phosphoria Formation of Derby field, Wind River basin, Wyoming, USA. The oil is sourced from the Permian Phosphoria Formation in the Idaho/Wyoming part of the thrust belt and migrated long distances into the central Wyoming (Kirschbaum *et al.*, 2007). The oil is characterised by Type II-S kerogen. The timing of generation and migration of the Phosphoria oil from the Idaho-Wyoming border has been proposed to be prior to the Laramide Orogeny (70 Ma) before it blocked the migration pathway (Sheldon, 1967; Stone, 1967; Kirschbaum *et al.*, 2007). The onset of generation for the Derby oil is considered to be similar to that of the Bighorn basin Phosphoria petroleum system (~ 200 Ma; Lillis & Selby, 2013). This oil has an asphaltene content of 6%.

The Federal oil (106.78°W, 42.86°N) is recovered from the Pennsylvanian Tensleep Formation of South Casper Creek field, Wind River basin, Wyoming, USA. Similar to the Derby oil, the Federal oil is also sourced from the Permian Phosphoria Formation, being generated from the Late Triassic (~ 200 Ma), but before the Laramide Orogeny (Kirschbaum *et al.*, 2007; Lillis & Selby, 2013). The oil is also considered to have migrated a significant distance (≥150 km). The Federal oil possesses an API gravity of 12°, sulphur content of 4.5% and asphaltene content of 12%.

The Viking-Morel oil (105.06°W, 44.58°N) is recovered from the Pennsylvanian-Permian Minnelusa Formation of Morel field, Powder River basin, Wyoming, USA. The oil is locally sourced from the Minnelusa Formation containing Type II medium sulphur kerogen (Clayton *et al.*, 1992). The timing of oil generation is not known, but is presumed to be during the Cretaceous. The oil has an API gravity of 25°, sulphur content of 3.3% and asphaltene content of 9%.

The Purisima oil (120.42°W, 34.72°N) is recovered from the Miocene Monterey Formation of Lompoc field, Santa Maria basin, California, USA. The oil is considered to have been generated during the last 5 million years from the Miocene Monterey Formation which is characterized by Type II-S kerogen (Isaacs & Rullkötter, 2001). The oil has

an API gravity of 22° and asphaltene content of 16%. It is observed that the oil sample contains water which cannot be removed completely by centrifuging.

The Persian oil is from a Cenomanian carbonate reservoir in the Persian Gulf. The oil source rock is probably of Cretaceous and/or Late Jurassic marine origin with Type II-S kerogen (Alsharhan & Nairn, 1997). This oil has a total asphaltene content of 6%.

The RM8505 oil is a Venezuelan crude oil. No further geological details of the origin are available from the provider NIST. The predominant source units of crude oil in Venezuela are the Upper Cretaceous (Cenomanian-Turonian-Coniacian, 100 – 86 Ma) La Luna Formation (mainly Type II kerogen) and its age equivalents, with only minor contributions from Palaeocene, Eocene and Miocene source rocks (James, 1990, 2000; Summa *et al.*, 2003). The majority of oil generation of the La Luna Formation is considered to have occurred since the Miocene (< 23 Ma), although oil generation is noted to have started as early as the Early Eocene (56 Ma) (James, 2000; Summa *et al.*, 2003). This oil has an asphaltene content of ~ 13% (Liu & Selby, 2018).

2.2 Sample preparation

For each oil sample, Re-Os measurements were made on the whole oil, *n*-heptane separated bulk asphaltene and maltene, the progressively precipitated fractions of asphaltene via the mixture of *n*-heptane and dichloromethane (DCM), and the asphaltene and maltene fractions separated by a series of *n*-alkane-DCM-methanol solutions.

Asphaltene and maltene were initially separated by a 40:1 *n*-heptane protocol from crude oils (Speight, 2004; Selby *et al.*, 2007). In brief, ca. 40 ml of *n*-heptane per gram of crude oil was thoroughly mixed with the crude oil. The mixture was put on a rocker overnight (for at least 16 hours) and then centrifuged for 20 minutes at 4000 rpm (revolutions per minute), equivalent of ca. 1600 g. The supernatant consisting of the *n*-heptane and soluble maltene fraction was decanted into a pre-weighed glass vial, and the *n*-heptane was evaporated at 80 °C to recover the maltene fraction for Re-Os analyses. The precipitated asphaltene at the bottom of the centrifuge tube was also collected into pre-weighed glass vial with ≤1 ml chloroform. The chloroform was evaporated at 60 °C to recover the asphaltene fraction. An aliquant of the bulk asphaltene (ca. 250 mg) was set aside for Re-Os analysis, the remaining asphaltene fraction was used for progressive precipitation experiments (see below).

The progressive precipitation of asphaltene was achieved by using a binary mixture of DCM as the solvent and *n*-heptane as the precipitant (Figure 1) (Nalwaya *et al.*, 1999; Kaminski *et al.*, 2000; Mahdaoui *et al.*, 2013). Precipitation of asphaltene occurs in response to the step-by-step increase of the percentage (5 volume % per step) of *n*-heptane in the binary mixture. The amount of asphaltene used for the progressive precipitation ranged between 2 and 4 g. The *n*-heptane-DCM mixture volumes are kept the same for every step (50, 200 and 250 ml for different samples, Table 1). The bulk asphaltene fraction was firstly dissolved in DCM which was followed by the addition of *n*-heptane. The mixture was then left on a rocker overnight and centrifuged at 4000 rpm for 20 minutes. After centrifuging, the supernatant was decanted and the precipitate, if there was any, was collected into pre-weighed glass

vials with ≤1 ml chloroform and dried at 60 °C. The DCM and *n*-heptane were extracted from the supernatant to recover the soluble fraction of asphaltene using a rotary evaporator (40 °C water-bath and 200 - 50 mBar pressure).The recovered soluble fraction of asphaltene would be used for the following step with 5% (volume) more of *n*-heptane in the DCM and *n*-heptane solution (Figure 1). The last steps used 100% *n*-heptane. Starting from an *n*-heptane: DCM ratio of 50:50, the first precipitations of the six bulk asphaltenes were observed on the ratio of 65:35 or 70:30 (Table 1). The asphaltene (g) to DCM (ml) ratios are generally from 0.01 to 0.02, with the exception of ~ 0.05 for the RM8505 sample.

Each of the same six crude oils was also separated into a series of asphaltene fractions and a series of maltene fractions with the *n*-alkane solutions, i.e. *n*-pentane, *n*-hexane, *n*-heptane, *n*-octane, *n*-nonane and *n*-decane (i.e. *n*-C_5, *n*-C_6, *n*-C_7, *n*-C_8, *n*-C_9 and *n*-C_{10}) using the protocol presented by Weiss *et al.* (2000) and applied by Georgiev *et al.* (2016). In brief, 3 ml DCM-methanol (93:7 v/v) was added to ~ 1 gram of oil to dissolve the oil. Then the *n*-alkane (40 ml/g oil) was added and the mixture was then put on a rocker overnight for at least 16 hours. The asphaltene was separated by centrifuging the mixture at 4000 rpm for 20 minutes. The same 3 ml DCM-methanol and 40 ml *n*-alkane procedure was repeated on the isolated asphaltene to remove any co-precipitates (Gürgey, 1998; Alboudwarej *et al.*, 2001; Álvarez *et al.*, 2015; Georgiev *et al.*, 2016). The *n*-alkane-DCM-methanol-asphaltene solution was left on a rocker overnight for at least 16 hours and then centrifuged. The precipitated asphaltene was removed to a pre-weighed glass vial using chloroform, and then evaporated at 60 °C. The supernatant was added to the supernatant from the first step and the *n*-alkane, DCM and methanol were removed using a rotary evaporator (30 - 70 °C water-bath and 400 - 30 mBar pressure) to fully recover the maltene fraction. The maltene was also collected with chloroform and placed into a pre-weighed glass vial, with the chloroform evaporated at 60 °C.

2.3 Re-Os analyses of the samples

The Re-Os analyses were conducted by Isotope Dilution – Negative Thermal Ionisation Mass Spectrometry (ID-NTIMS) at the Durham Geochemistry Centre at Durham University in the Source Rock and Sulfide Geochronology and Geochemistry, and Arthur Holmes Laboratories (Selby *et al.*, 2007). With the exception of asphaltene fractions that dried to a solid (i.e. could be powdered in an agate pestle and mortar), all samples were loaded into Carius tubes in ≤1 ml of chloroform or DCM, which was then evaporated at 60˚C overnight. The sample was digested by inverse *aqua regia* (3 ml 12 N HCl + 6 ml 15.5 N HNO_3) and equilibrated with a mixed tracer solution of ^{185}Re and ^{190}Os at 220°C for 24 hours. The Os was extracted from the digested sample by solvent extraction using chloroform, and back extracted in 3 ml of 9N HBr, and then further purified by CrO_3-H_2SO_4-HBr micro-distillation. The Re was purified by HCl-HNO_3 based anion exchange chromatography. Both the Re and Os purified fractions were loaded on Ni and Pt wire filaments, respectively, and measured for their isotopic composition by NTIMS, using static collection by Faraday cups and peak-hopping mode on a secondary electron multiplier, respectively.

The total Re-Os measurement procedural blanks during the study are 1.63 ± 0.67 picograms for Re and 65 ± 13 femtograms for Os, with an average ^{187}Os/^{188}Os of 0.23 ± 0.02 (2 SD, n = 8). The blank represents up to 0.12 and 0.93 % of the Re and Os budget of the asphaltene fractions, respectively. For the maltene fraction, the blank Re and

Os concentration represents, on average, 0.7 and 3.0 % and up to 3.8 and 9.2 %, respectively (Supplementary Material 1 & 2). The average $^{187}Os/^{188}Os$ value of the in-house Os standard, DROsS, is 0.1611 ± 0.0004 (1SD, n = 126). The average $^{185}Re/^{187}Re$ value of the Re standard, ReStd, is 0.5989 ± 0.0019 (1SD, n = 116). The $^{185}Re/^{187}Re$ value of 0.5974 (Gramlich *et al.*, 1973) is used for the Re sample mass fractionation correction. Data reduction includes the instrumental mass fractionation, isobaric oxygen interference and contribution of blanks and the tracer solution. The final expanded (k = 2) combined standard uncertainties of the results include the fully propagated of uncertainties of sample-weighing, tracer calibration, blank abundances and isotope compositions, and the intermediate precision of the results of repeated measurements on the Re and Os reference solutions.

3 Results

3.1 The progressive precipitation of asphaltene and the separation of crude oil by *n*-alkanes

The six crude oils used in this study possess between 5.7 and 16.1% bulk asphaltene as separated by *n*-heptane (Table 1). Maltene fractions were only partially collected for Re-Os analyses for most oil samples, thus no maltene mass fractions are available. However, RM8505 has been thoroughly studied in regard to its asphaltene and maltene yields in a previous study (Liu & Selby, 2018).

For the progressive precipitation of asphaltene via *n*-heptane-DCM solutions, four of the samples precipitated the first fractions of asphaltene from an *n*-heptane-DCM ratio of 65:35 (Federal, Persian, Purisima and Viking Morel). Asphaltenes of both the Derby and RM8505 oil first precipitated with an *n*-heptane-DCM ratio of 70:30. The progressively precipitated fractions of the asphaltene account for 2 to 22% of the original bulk asphaltene, with the exception of the first precipitation of RM8505, which accounts for 54% of the bulk asphaltene (Table1; Figure 2). From 7 to 23% of the original asphaltene are still soluble in 100% *n*-heptane at the last step of the progressive precipitation. All of the progressively precipitated asphaltene fractions account for ca. 96 to 102% of the mass of the originally employed bulk asphaltene for the six samples (Table 1). The physical appearance of the fractions of asphaltene changes gradually from hard shiny black particles to amorphous dull brown powder and highly viscous fluids (the last 100% *n*-heptane soluble fraction) throughout the progressive precipitation, which is identical to what has been observed by previous studies, e.g., Nalwaya *et al.* (1999) and (DiMarzio *et al.*, 2018).

Four of the six oils (Derby, Federal, Viking Morel, Persian) separated using a *n*-alkane-DCM-methanol solution show a general decrease in asphaltene yields with the increase of *n*-alkane chain length from *n*-C_5 to *n*-C_7, with similar yields from *n*-C_7 to *n*-C_{10} (Figure 3; Table 2). The exceptions are for the oil samples Purisima and RM8505, which show a decrease in asphaltene yields from *n*-C_5 to *n*-C_7, with a slight increase for *n*-C_8 and lower values for *n*-C_9 that are similar to yields of *n*-C_7, and finally show a greater yield for *n*-C_{10} (Table 2; Figure 3). The majority of the asphaltene yields from the *n*-alkane-DCM-methanol solutions are lower than those obtained using solely *n*-heptane (cf. Tables 1 and 2), e.g. *n*-pentane 10.6% and *n*-heptane 7.8% asphaltene yields for the Federal oil with the

application of DCM-methanol versus 11.9% asphaltene obtained solely by *n*-heptane. The difference in asphaltene yields is attributed to the use of DCM-methanol, especially the DCM. The maltene yields are almost identical with a slight increase. in general, from *n*-C_5 to *n*-C_{10} for the Persian, RM8505 and Viking-Morel oil samples: ~ 70% for Persian oil, ~ 88% for the RM8505 oil and ~ 75% for Viking-Morel oil (Figure 3; Table 2). For the Derby sample, the maltene yields are around 82% from *n*-C_7 to *n*-C_9 with a slight increase to 84% using *n*-C_{10} and as high as 10% variations using *n*-C_5 and *n*-C_6. For the Federal sample, ca. 14% increase in the maltene yields is observed when using *n*-C_6 compared to using *n*-C_5. From *n*-C_6 to *n*-C_{10} the maltene yields of Federal oil are approximately 80%. Variation of maltene yields from ca. 35% to 50% is observed for Purisima oil owing mostly to the water contents in the crude oil.

The less than 100% total yields of asphaltene and maltene can be accounted for by the loss of any volatile phase and sometimes water in the oil, plus weighing error propagation. For example, 4.4% of the mass was lost by heating 0.3 g of RM8505 crude oil at 80 °C for 10 days (Liu & Selby, 2018). The reduced loss of RM8505 in this study (4.2%) compared to the average loss (7.9%) during the *n*-heptane separation of asphaltene and maltenes by Liu and Selby (2018) on the same oil could be attributed to the use of rotary evaporator rather than heating via a hot plate to recover the maltene from *n*-heptane and *n*-alkane-DCM-methanol solutions. Further, water present in the oil samples, e.g. Purisima, may have only been partially removed by centrifuging. As such variable amounts of water present in the oil may have contributed to the inconsistency of the asphaltene and maltene yields and mass balance of the separation.

3.2 Re and Os elemental concentrations and distribution in the fractions of oil

3.2.1 Re-Os data of whole oil and asphaltene and maltene separated by *n*-heptane

The six crude oil samples contain relatively large ranges in Re and Os concentration and isotopic composition. Data are reported in Tables 3-8. The six whole oils possess 2 to 12 ppb Re and 12 to 173 ppt Os. The bulk separated asphaltene fractions contain 15 to 164 ppb Re and 147 to 1826 ppt Os, whereas the bulk separated maltenes contain only 0.3 to 1.6 ppb Re and 4 to 31 ppt Os.

3.2.2 Re-Os data of the progressively precipitated fractions of asphaltene

During the progressive precipitation of asphaltene using the *n*-heptane-DCM protocol, the earlier precipitated fractions generally contain higher Re and Os concentrations (Table 3- 8; Figures 4 - 5). The exceptions are the Re and Os concentrations for the first precipitated fractions of the Persian and Viking-Morel oil samples and the Re concentration for the first precipitated fraction of the Purisima sample. A large portion of the first precipitated fraction of Persian asphaltene does not dissolve in $CHCl_3$ during transfer to the Carius tube for Re-Os analysis, This $CHCl_3$ non-soluble material appears as both a white powder and white needles. This material could be salts or wax which could possess limited Re and Os.

In general, the concentrations of the most Re and Os enriched first or second asphaltene precipitates (i.e. at *n*-heptane-DCM ratios of 65:35 and/or 70:30) are 1.4 to 2.7 times that of the original bulk asphaltene isolated solely by

n-heptane. The Re and Os concentrations of the precipitates of the last steps of the progressive precipitation are 0.3 to 0.6 times that of the original bulk asphaltene. The Re and Os concentrations of the 100% *n*-heptane soluble fractions are lower than all the precipitated fractions, but higher than the maltenes isolated solely by *n*-heptane. It is observed that the Re and Os concentrations decrease in similar ways for the Federal, Persian and Viking-Morel samples with the Re decreasing slightly faster than Os. For the Derby sample, Re and Os decrease at the same rate. For the RM8505 sample, the Re decreases much faster than Os. For the Purisima sample, Os decreases faster than Re.

The mass balance of the Re and Os concentrations during the progressive precipitation is calculated (Table 9). The total Re, ^{192}Os (representing unradiogenic Os) and radiogenic ^{187}Os of all the fractions of asphaltene account for approximately 100% of their contents in the original bulk asphaltenes for the Derby, RM8505 and Viking-Morel samples. The less than 100% recovery rates of the Federal and Persian samples could be accounted for by the weighing errors of the fractions and possible loss of sample during the analytical protocol, especially for the Re and Os more abundant fractions. The 101% recovered Re and ~ 110% recovered ^{192}Os and ^{187}Os of the Purisima could be the contamination of Os from the sample preparation and/or Re-Os measurement processes, or it could be related to weighing error of the Re and Os more abundant fractions and loss of Re.

3.2.3 Re-Os data of the *n*-alkane-DCM-methanol separated asphaltenes and maltenes

Compared to the asphaltene and maltene fractions separated solely by *n*-heptane, the asphaltenes and maltenes separated by the *n*-alkanes plus DCM and methanol protocol are generally more enriched in Re and Os, with the exception of asphaltenes isolated using *n*-C_5 and *n*-C_6 from the Derby oil (Tables 3, 10 and 11; Figures –6 - 8). The enhanced concentrations are attributed to the reduced yields of asphaltene. The Re and Os concentrations of *n*-alkanes asphaltenes can be as high as 1.6 times that of the *n*-heptane only isolated asphaltenes (e.g., in the case of *n*-C_7 asphaltene from RM8505 and *n*-C_9 asphaltene from Purisima oil). The Re and Os concentrations of the *n*-alkane-DCM-methanol isolated maltenes can be as high as 5 (RM8505, *n*-C_{10}) and 3 (Viking-Morel, *n*-C_{10}) times that of the *n*-heptane isolated maltene fractions.

The Re and Os concentrations of the asphaltenes generally increase with the increase in chain length of the precipitant *n*-alkane except for the Viking-Morel sample, especially from *n*-C_5 to *n*-C_7 (Table 10; Figure 6). For almost all of the six oil samples, the Re and Os concentrations of the maltenes increase with the increase in chain length of the precipitant *n*-alkanes (Table 11; Figures –7 - 8), except for the Derby and Federal samples from *n*-C_8 maltene onwards, which are very similar. The mass balance of the Re and Os for the separation of asphaltene and maltene using the *n*-alkane-DCM-methanol solution is calculated according to their mass fractions (Supplementary Material 1). The total Re and Os contents of the pairs of asphaltene and maltene are in general comparable to those of the original whole oil with the differences generally within 10% for the Derby, Federal, Persian and Viking-Morel oil samples despite the various loss of sample. The total Re and Os contents of the pairs of asphaltene and maltene of the Purisima oil are variable and show up to 43% Re and 33% Os less than the measured whole oil, which are not surprising if consider the variable loss of up to 55% of sample during separation which could relate to the low Re

and Os concentration within water and volatile fractions. The total Re and Os contents of the asphaltene and maltene pairs of RM8505 are ~2.2 to 2.8 ppb Re and ~28 to 30 ppt Os. These values are higher than the whole oil analyzed previously in this laboratory (~1.7 to 2.2 ppb Re and ~21 to 27 ppt Os, n = 18; Liu and Selby (2018)), however, similar to the two analyses reported by Georgiev *et al.* (2016) (~2.3 ppb Re and ~31 and 29 ppt Os). This may be explained by the heterogeneity of crude oil Re-Os systematics (Liu & Selby, 2018).

3.3 Re-Os isotopic systematics

3.3.1 Re-Os isotopic compositions of whole oil and asphaltene and maltene separated by *n*-heptane

The six oil samples exhibit a large spread in Re-Os isotopic compositions (Tables 3 - 8; Figures 4, 5, 9 and 10). The $^{187}Re/^{188}Os$ values of the six oils vary from 454 (RM8505) to 1589 (Persian) and the $^{187}Os/^{188}Os$ compositions vary from 0.96 (Purisima) to 4.22 (Federal). The asphaltene $^{187}Re/^{188}Os$ values and $^{187}Os/^{188}Os$ compositions, although similar, are generally higher and more radiogenic than that of the whole oil (Tables 3 - 8; Figures 4, 5, 9 and 10). In contrast, the maltene fractions possess lower $^{187}Re/^{188}Os$ values and less radiogenic $^{187}Os/^{188}Os$ compositions than those of the whole oil and asphaltenes (Tables 3 - 8; Figures 4, 5, 9 and 10). The $^{187}Re/^{188}Os$ values of the bulk-separated six asphaltene samples are from 496 (Viking-Morel) to 2066 (Persian) and the $^{187}Os/^{188}Os$ compositions vary from 0.98 (Purisima) to 4.23 (Federal). The $^{187}Re/^{188}Os$ values of the bulk separated six maltene samples vary from 183 (RM8505) to 594 (Federal) and the $^{187}Os/^{188}Os$ compositions vary from 0.71 (Purisima) to 3.59 (Federal).

3.3.2 Re-Os isotopic compositions of the progressively precipitated fractions of asphaltene

The Re-Os isotopic compositions of the progressively precipitated asphaltene fractions from *n*-heptane-DCM solutions exhibit unique characteristics for each of the six samples (Tables 3 - 8; Figures 4, 5, 9 and 10). For example, both of the $^{187}Re/^{188}Os$ and $^{187}Os/^{188}Os$ are similar for the Derby samples except for the last two fractions (Figure 4). The Re-Os compositions for the RM8505 samples show a linear-like distribution in $^{187}Re/^{188}Os$-$^{187}Os/^{188}Os$ space (Figure 10), i.e. simultaneous decrease of $^{187}Re/^{188}Os$ and $^{187}Os/^{188}Os$ throughout the progressive precipitation process (Figure 5). For the Viking-Morel samples, the $^{187}Re/^{188}Os$ decreases and the $^{187}Os/^{188}Os$ remains almost constant throughout the progressive precipitation.

The expected $^{187}Re/^{188}Os$ and $^{187}Os/^{188}Os$ for the original bulk asphaltenes calculated from the progressively precipitated fractions of asphaltenes for Derby, RM8505 and Viking-Morel samples are identical with their bulk asphaltenes (Table 9). Together with their good mass balance presented in Section 3.2.2, chances of high blank or contamination contribution are low for these samples.

The expected $^{187}Re/^{188}Os$ and $^{187}Os/^{188}Os$ of Persian samples are slightly lower than those of the bulk asphaltene's which may suggest higher than normal blank with less radiogenic Os than the samples. The Persian oil shows a negative distribution in $^{187}Re/^{188}Os$-$^{187}Os/^{188}Os$ space (Figure 4 and Figure 9), i.e. decreasing $^{187}Re/^{188}Os$ and increasing $^{187}Os/^{188}Os$ throughout the progressive precipitation.

The expected $^{187}Re/^{188}Os$ for Federal sample and $^{187}Os/^{188}Os$ for Purisima sample are identical to the measurement on their original asphaltenes. Throughout the progressive precipitation, the $^{187}Re/^{188}Os$ for Federal samples decrease in general similar to the RM8505 and Viking-Morel samples. The $^{187}Os/^{188}Os$ for Purisima samples are similar, as shown for the Derby and Viking-Morel samples. However, poor there is poor agreement between the expected and measured $^{187}Os/^{188}Os$ for Federal sample and $^{187}Re/^{188}Os$ for Purisima sample (Table 9). Throughout the progressive precipitation, the $^{187}Os/^{188}Os$ for Federal samples apparently vary and are lower than the bulk asphaltene $^{187}Os/^{188}Os$. This is could be the result of contamination by less radiogenic Os or loss of ^{187}Os. The $^{187}Re/^{188}Os$ for Purisima sample increase throughout the progressive precipitation, which is different with all the other five samples in this study. This could be a true trend, or maybe relate to the undervaluation of Re or overvaluation of Os of the first few fractions.

3.3.3 Re-Os isotopic compositions of asphaltenes and maltenes separated by *n*-alkanes

The $^{187}Os/^{188}Os$ values of the asphaltenes separated by the *n*-alkane-DCM-methanol protocol for the same oil sample are very similar to each other and to that of the bulk separated asphaltene by *n*-heptane (Figures 9 – 10; Table 10). The exception is the Persian samples for which the variations of $^{187}Os/^{188}Os$ are beyond the measurement uncertainties and the $^{187}Os/^{188}Os$ are lower than obtained for the *n*-heptane asphaltene. There is also a trend of increasing $^{187}Os/^{188}Os$ for the RM8505 samples although they are within measurement uncertainties. The $^{187}Re/^{188}Os$ values of the asphaltene fractions are variable with the highest values to be from 105% to 112% of the lowest values. These values are higher than the whole oils and the *n*-heptane only separated asphaltenes for four of the six samples.

The $^{187}Os/^{188}Os$ compositions of the maltene fractions separated by the *n*-alkane-DCM-methanol protocol for the same oil sample are, including uncertainties, very similar (Figures 7 – 10; Table 11). These values are lower than that of the whole oil. A trend to slightly more radiogenic $^{187}Os/^{188}Os$ values for the maltene fractions especially recovered from *n*-C_5 to *n*-C_7 solutions is observed for most oils, with the exception of the Viking-Morel oil sample (Figures 7 - 8). Most of the $^{187}Re/^{188}Os$ values of the maltene fractions are higher than that of the bulk maltene from the *n*-heptane separation, but lower than the values for the whole oil. A general trend increasing $^{187}Re/^{188}Os$ values is observed for the maltene fractions precipitated from *n*-C_5 to *n*-C_8, *n*-C_9 and even *n*-C_{10}.

The expected whole oil $^{187}Re/^{188}Os$ and $^{187}Os/^{188}Os$ calculated from the asphaltene and maltenes are basically identical to the results of Re-Os measurements on the whole oils (Supplementary Material 1). The expected $^{187}Os/^{188}Os$ of Federal and RM8505 samples are lower than the measured whole oils (ca. 3.95 vs 4.22 and ca. 1.4 vs 1.54, respectively). The expected Persian whole oil $^{187}Re/^{188}Os$ are higher than the measured result on whole oil while the expected Purisima $^{187}Re/^{188}Os$ are lower than the measured result. Contaminations and weighing errors can play more significant role on these small samples with regard to sample mass and Re and Os concentrations. Both of

the expected whole oil $^{187}Re/^{188}Os$ and $^{187}Os/^{188}Os$ match well with the measured values on the whole oils for Derby and Viking-Morel samples.

In fact, in terms of mass balance the Re-Os isotope data of the whole oil should be on the line defined by the asphaltene and maltene fractions, if measured precisely and accurately. Maltene is more difficult to measure than the asphaltene and whole oil – blank correction or other errors play a more significant role for maltene. Besides accurate and precise measurements, heterogeneity can also lead to the deviation of crude oil data point from the line defined by the asphaltene and maltene (Liu & Selby, 2018) which is another form of the multiple crude oil samples methodology. For most of the samples in this study, the whole oil data points are between the asphaltene clusters and maltene clusters (Figures 9 – 10).

4 Discussion

4.1 The residence of Re and Os in crude oil and asphaltene

4.1.1 Asphaltene is the main carrier of Re and Os of crude oil

The Re-Os analyses of the asphaltene and maltene fractions separated by both solely *n*-heptane and *n*-alkane-DCM-methanol solutions in this study support that the asphaltene is the main carrier of Re and Os in the majority of crude oils (Selby *et al.*, 2007; Rooney *et al.*, 2012; Cumming *et al.*, 2014; Georgiev *et al.*, 2016; DiMarzio *et al.*, 2018; Liu & Selby, 2018). When separated by solely *n*-heptane, the asphaltene fractions of the six oil samples in this study account for ≥ 78% Re (of Derby oil sample) and ≥ 73% Os (of Derby oil sample) of the original whole oils (Supplementary Material 2). These values are lower than previously reported (> 90% Re and 83% Os; Selby et al., 2007). When separated by *n*-alkane-DCM-methanol solutions, the asphaltene fraction accounts for more than 52% Re (of Purisima oil sample separated with *n*-heptane) and 58% Os (of Federal oil sample separated with *n*-decane; Supplementary Material 1), which are comparable to the division of the Streppenosa asphaltenes in Georgiev *et al.* (2016), i.e. 55-79% Re and Os.

However, the remaining *n*-heptane maltene fractions, which account for the majority of the mass of whole oil, although the exact mass fractions were not obtained for the majority of the six oil samples, contain much less Re and Os than the asphaltenes. Similarly, the *n*-alkane-DCM-methanol maltenes contain less Re and Os than their corresponding asphaltenes (Supplementary Material 1), although generally more than the *n*-heptane maltene fractions.

4.1.2 The state of molecules containing Re and Os in crude oil and the role of asphaltene

Multiple heteroatomic complexes and stable porphyrins are proposed to be the hosts of Re and Os in crude oil (Selby & Creaser, 2003; Miller, 2004; Selby *et al.*, 2007). The amounts and kinds of these Re and Os containing compounds in the crude oils should also depend on the origin, maturity and migration and alteration processes, etc. Based on the understanding of asphaltene aggregation behaviour, we propose that in the DCM solution of asphaltene

and in the crude oil, Re and Os can both exist as metals bound by multiple heteroatomic complexes (including metalloporphyrins and single asphaltene molecules) in free state and such metal complexes associated with asphaltene aggregates by occlusion and adsorption.

It is possible that the Re and Os bearing species in crude oil can be adsorbed and occluded into the asphaltene aggregates like many other compounds (Mujica *et al.*, 2000; Liao *et al.*, 2005; Liao *et al.*, 2006a, 2006b; Liao *et al.*, 2009; Acevedo *et al.*, 2012; Derakhshesh *et al.*, 2013; Zhao *et al.*, 2013; Liu *et al.*, 2015; Castillo & Vargas, 2016; Snowdon *et al.*, 2016; Evdokimov *et al.*, 2017). The molecules absorbed at the periphery of asphaltene aggregates, i.e. those that are loosely packed, are liable to be exchanged with the outside bulk phase. This is in contrast to the tightly bound molecules of the interior of the asphaltene aggregate that are occluded and cannot be exchanged and can remain stable and be preserved in crude oil over geological time (Liao *et al.*, 2005). The occluded molecules can be preserved and protected from secondary alteration of crude oil through geological time, e.g. biodegradation (Liao *et al.*, 2006a; Snowdon *et al.*, 2016; Cheng *et al.*, 2017). The occluded molecules can be influenced by thermal stress like the absorbed molecules, but their interchange is considered to be limited. This means that in the asphaltene aggregates the loosely packed Re and Os bearing compounds may be liable to exchange with the surrounding molecules, whereas the tightly packed occluded Re and Os molecules could be well-preserved through geological times and geological changes.

Consistent with previous studies (Mahdaoui *et al.*, 2013; DiMarzio *et al.*, 2018), we observe that the progressive precipitation separates different chemical groups of bulk asphaltene with different Re and Os concentrations for the six samples. Specifically, the earlier precipitated fractions have higher Re and Os concentrations, except the first precipitated fractions of Persian and Viking-Morel oils (Figures 4- 5). Polarity, aromaticity, aggregate/molecular/aromatic core sizes and mainly van der Waals interactions have been shown in several studies to define the differences among the separated fractions of asphaltene (Buckley & Fuels, 1999; Groenzin *et al.*, 2003; Porte *et al.*, 2003; Speight, 2004), however, how these properties relate to Re and Os concentrations remains unknown. Nevertheless, other possible reasons for the observed decrease of Re and Os concentrations in this study could be the decrease in the concentration of the Re and Os carrying molecules and the decreased ability of asphaltene molecules to co-precipitate with these molecules. However, such an assumption requires that the Re and Os are not linked with a given fraction of asphaltene prior to precipitation, In this case, the isochron using such a fractionation is no longer meaningful.

4.2 Implications from the Re-Os isotopic systematics of various fractions of crude oil

For all of the six crude oil samples in this study, differences in the $^{187}Re/^{188}Os$ and $^{187}Os/^{188}Os$ compositions exist among the whole oil, bulk asphaltene and maltene fractions separated solely by *n*-heptane, progressively precipitated asphaltene fractions by *n*-heptane-DCM solutions, and the asphaltene and maltene fractions separated by *n*-alkane-DCM-methanol solutions (Figures 4, 5 and 7 - 10).

The different decrease rates of the Re and Os concentrations are also reflected in the $^{187}Re/^{188}Os$ ratios (Figures 4 - 5), except for the Derby samples for which the first six fractions have similar $^{187}Re/^{188}Os$ values. The $^{187}Re/^{188}Os$

values generally decrease throughout the progressive precipitation or for a few fractions, for the Federal, Persian, RM8505 and Viking-Morel oil samples (Tables 3 - 8; Figures 4 - 5). In contrast, the $^{187}Re/^{188}Os$ values increase throughout the progressive precipitation for the Purisima oil sample, with the exception of the last soluble fraction in 100% *n*-heptane. Despite the imperfect mass balance of Federal, Persian and Purisima samples and the similar $^{187}Re/^{188}Os$ of Derby samples, difference in $^{187}Re/^{188}Os$ among the progressively precipitated fractions of asphaltenes is clearly shown in this study by at least the RM8505 and Viking-Morel samples. This indicates the presence of different Re and Os bearing complexes which leads to the discrepancy of their behaviour throughout the progressive precipitation.

Although slight differences exist, the $^{187}Os/^{188}Os$ compositions of the progressively precipitated asphaltene fractions are quite similar (overlapping within uncertainty) for each of the Derby, Purisima, and Viking-Morel samples (Figures 9 - 10). The similarity of the $^{187}Re/^{188}Os$ and $^{187}Os/^{188}Os$ of the progressively precipitated fractions of Derby asphaltene (Table 3; Figure 9) may suggest a complete exchange of the Re and Os bearing entities in crude oil. The parent ^{187}Re is expected to co-vary with its daughter ^{187}Os. However, the decrease of the $^{187}Re/^{188}Os$ of Viking-Morel asphaltene fractions is not coupled with apparent decrease of the $^{187}Os/^{188}Os$. This relationship may be due to the oil being too young or the spread of $^{187}Re/^{188}Os$ values of the fractions being too limited to generate discernible differences of $^{187}Os/^{188}Os$ among the fractions of asphaltene. However, it could also be that the radiogenic ^{187}Os decouples from the parent ^{187}Re and behaves similarly to the other Os atoms of the sample. Although being compromised by the imperfect mass balance, the Persian and Purisima samples may also exhibit evidence of the decoupling of radiogenic ^{187}Os from the parent ^{187}Re. The Persian samples show decreasing $^{187}Re/^{188}Os$ with increasing $^{187}Os/^{188}Os$, whereas the Purisima samples show increasing $^{187}Re/^{188}Os$ with unchanging $^{187}Os/^{188}Os$ throughout the progressive precipitation.

Coupled with the decrease in $^{187}Re/^{188}Os$ values with the progressive precipitation is also a trend to less radiogenic $^{187}Os/^{188}Os$ compositions for the RM8505 oil sample, which is also true for the Federal sample in general (Figures 9 - 10). As such, the radiogenic ^{187}Os is proportional to the parent ^{187}Re rather than the inherent Os. This behaviour suggests that the majority of the radiogenic ^{187}Os is likely still in the same/similar complexation location as the parent ^{187}Re following the beta decay. This scenario is most likely to happen when the Re is predominantly housed tightly in the asphaltene aggregates and protected from any exchanges by occlusion, rather than in the adsorbed molecules where exchange of ions is labile, or in the free metalloporphyrins or other heteroatomic complexes. In contrast, the Re in the Derby, Purisima and Viking-Morel oil samples could possibly be predominantly in the multiple heteroatomic complexes as free molecules.

The unique characteristics exhibited by each of the six samples can possibly be attributed to their unique nature or the influence of separation based on experimental procedures. The nature of crude oil includes the organic matter type, maturity and alteration processes, etc., which may determine whether the Re and Os will be in the closed

asphaltene aggregates or in the free molecules. The influence of experimental procedures can be examined with repeated experiments taken on the same sample, which is beyond the scope of this present study.

4.3 Implications for Re-Os geochronology from the separation of crude oil

4.3.1 The Re-Os geochronology information obtained from the oil fractions of this study

In the study of Georgiev *et al.* (2016), the Re-Os data of the fractions of a single oil were interpreted to determine Re-Os ages which define the timing of oil generation. Here, we discuss the application of the Re-Os isotope systematics of the asphaltene and maltene fractions separated by *n*-alkane-DCM-methanol solutions for geochronology to the six crude oil samples in this study. In addition, we discuss the Re-Os geochronology with the *n*-heptane separated fractions (whole oil, bulk asphaltene, bulk maltene) and the progressively precipitated fractions of asphaltene by *n*-heptane-DCM solutions. Combinations of the progressively precipitated fractions of asphaltenes were also explored for geochronology – meaning in the Re-Os data set more than two samples define a best-fit line in $^{187}Re/^{188}Os$ vs $^{187}Os/^{188}Os$ space (Figure 9 - 10). The regression analysis using *Isoplot* v. 4.15 (Ludwig, 2012) of the Re-Os isotopic data for these fractions for all oil samples are listed in Table 12 - 13.

No matter what combination of the crude oil fraction Re-Os data is used, no meaningful geological dates can be obtained systematically for every oil sample (Table 12 - 13). This means that even if a set of fractions of a crude oil can yield a meaningful age, it is not guaranteed for other crude oils with same combination of the fractions of crude oil. Furthermore, no consistent Re-Os ages can be obtained for a crude oil by all the shown combinations of the fractions in Tables 12 - 13. Additionally, the large uncertainty of most of the obtained dates also reduces their credibility. The most precise date values are obtained by the progressively precipitated fractions of asphaltene of sample RM8505 (98.4 ± 9.5 Ma; Table 12), by the asphaltenes and maltenes plus whole oil (30.1 ± 4.3 Ma; Table 13) and by the maltene fractions (27.3 ± 8.7 Ma; Table 13) separated by *n*-alkane-DCM-methanol solutions for the Purisima sample. For both oils the dates obtained are close to the deposition age of their source rocks (James, 1990, 2000; Isaacs & Rullkötter, 2001; Summa *et al.*, 2003), respectively, rather than the timing of oil generation. The Re-Os data of a few fractions of the progressively precipitated asphaltene fractions of Derby and Purisima samples define Re-Os dates of 170 ± 50 Ma and 5.5 ± 2.5 Ma, respectively, which are close to their known (Lillis & Selby, 2013) or estimated oil generation age. However, such combinations cannot yield geologically meaningful Re-Os ages for the other samples of this study. The dates yielded from the asphaltene and maltene (*n*-alkane-DCM-methanol) fractions plus whole oil for the Derby (96 ± 43 Ma) and Federal (67 ± 22) samples seem to be close to their possible oil generation age (before Laramide Orogeny, 70 Ma; Sheldon, 1967; Stone, 1967; Kirschbaum *et al.*, 2007), where the date (83 ± 20 Ma) determined for the RM8505 samples is close to both the potential source rock age (La Luna Formation; Cenomanian-Turonian-Coniacian, 100 – 86 Ma) and the earliest oil generation age (James, 2000; Summa *et al.*, 2003).

4.3.2 Implications for Re-Os geochronology utilizing the progressive precipitation of asphaltene

The observation of the similar Re/Os and $^{187}Os/^{188}Os$ for the majority of the asphaltene fractions (Mahdaoui et al., 2013) led to the conclusion that the sequential loss of asphaltene in natural petroleum systems will not greatly change the Re-Os isotopic systematics of crude oil, and thus will not impede the application of Re-Os geochronology on petroleum samples. In contrast, changes of both $^{187}Re/^{188}Os$ and $^{187}Os/^{188}Os$ compositions, either slightly or appreciably, are observed for most of the six samples of this study during the progressive precipitation with similar mixture of DCM and *n*-heptane versus DCM and *n*-pentane for some samples in Mahdaoui *et al.* (2013). In the situation for which a difference exists in the $^{187}Re/^{188}Os$ and/or $^{187}Os/^{188}Os$ composition among the solubility classes of asphaltene, the precipitation of fractions will lead to the change of $^{187}Re/^{188}Os$ and/or $^{187}Os/^{188}Os$ compositions of the remaining oil. The effect of precipitation will depend on the degree of the loss of asphaltene, the relative concentrations of Re and Os in the precipitates to the remaining fraction and how different the isotopic systematics are between the two. A similar observation is also made by (DiMarzio *et al.*, 2018), who showed for an oil sample from Italy, that the progressive precipitation of asphaltenes changes the $^{187}Re/^{188}Os$ of a heavy crude oil.

The establishment of an isochron with the fractionation of a single asphaltene sample is conditioned on the premise that the exchange of Re and Os among the fractions of asphaltene has never happened, i.e. there are closed reservoirs with regard to Re and Os within the asphaltene with identical initial $^{187}Os/^{188}Os$, and the fractionation protocol can cleanly separate these reservoirs. The decay of ^{187}Re to ^{187}Os should also be constrained by these reservoirs. This is only the case when all the Re and Os are occluded and protected from exchange in asphaltene aggregates. This situation will yield the Re-Os age of the asphaltene aggregates formation. If Re and Os are predominantly in the forms liable to exchange among asphaltene fractions, i.e. there is no closed reservoir, the zero age will be maintained as long as the exchange continues. In this case, precipitation of asphaltene may trigger the Re-Os chronometer. But if we are not sure of the occurrence of exchange and to what extent the exchange is, the interpretation of any Re-Os dates obtain by the fractions of asphaltene may be false. Furthermore, the Re-Os systematics within crude oil could also be affected by alteration. This should be taken into consideration when evaluating the validity of Re-Os dates from fractions of a single oil.

4.3.3 Implications for Re-Os geochronology from the asphaltene and maltene fractions separated by *n*-alkane-DCM-methanol solution

The asphaltene yields are shown to decrease with the increase of *n*-alkane C number in some studies (Buenrostro-Gonzalez *et al.*, 2004; Georgiev *et al.*, 2016). However, in some other studies (Figure 1, Mitchell & Speight, 1973; Figure 6, Corbett & Petrossi, 1978) and this study, the asphaltene yields decrease from *n*-C_5 to *n*-C_7, and then level off from approximately *n*-C_7 onwards to *n*-C_{10}. The unchanging yields reduce the possibility of creating spread in Re-Os isotopic ratios of the asphaltenes (Table 10) as well as the maltenes (Table 11; Figures 7 – 8). The maltene yields vary according to the change of asphaltene yields, the loss of volatile fractions and the influence of water contents (e.g. the Purisima sample). The variation of Re-Os isotopic ratios of the maltenes depend on the transfer of the reduced asphaltene yields with different Re-Os isotopic ratios into the maltene fractions.

Additionally, the different asphaltene yields have limited influence on the asphaltene Re-Os elemental and isotopic systematics. When the asphaltene yields decrease, the Re and Os concentrations of the asphaltenes increase with the $^{187}Os/^{188}Os$ remaining almost unchanged with the maximum/minimum for each oil to be 100.2%, 100.8%, 106.8%, 101.7%, 103.8% and 100.2%, respectively, and the $^{187}Re/^{188}Os$ show relatively small change with the maximum/minimum for each oil to be 104.9%, 104.9%, 105.8%, 111.7%, 106.2% and 107.6%, respectively. As stated in section 4.3.1 and shown in Figures 9 – 10 and Table 13, the $^{187}Re/^{188}Os$ and $^{187}Os/^{188}Os$ of the *n*-alkane asphaltene fractions for five of the six samples cannot define a meaningful Re-Os age. These asphaltenes yield close to 0 ages, which is the results of their similar $^{187}Os/^{188}Os$, with large uncertainties. The exception is for the RM8505 samples yielding an imprecise age of 65 ± 47 Ma which is close to the oil generation age (James, 2000; Summa *et al.*, 2003).The change in the Re-Os elemental and isotopic systematics of the maltene fractions by different *n*-alkane is more prominent than for the asphaltene fractions (Table 11; Figures 7 – 10). This is because the maltene fractions normally contain much less Re and Os than the asphaltene, leaving them easier to be affected by the change of components. The variation of maltenes' isotope composition for the six oil samples, expressed as maximum/minimum, are 122.4%, 139.3%, 177.2%, 206.6%, 182.4% and 119.5%, respectively for $^{187}Re/^{188}Os$ and 107.9%, 116.6%, 120.4%, 148.3%, 119.3% and 103.6%, respectively for $^{187}Os/^{188}Os$ using different *n*-alkanes as precipitant. However, only the Purisima maltene fractions yield a Model 1 best-fit line giving a Re-Os date of 27.3 ± 8.7 Ma, which is close to the age of the source rock (Table 13; Figure 10). None of the remaining maltene fractions yield any meaningful Re-Os dates (Table 13).

The asphaltenes and maltenes plus whole oil of Purisima and RM8505 samples define best-fit lines giving Re-Os dates of 30.1 ± 4.3 Ma and 83 ± 20 Ma, respectively which are close to the ages of their source rocks (Table 13). Same combinations of samples define a Re-Os date covering the end of the generation age for the Derby and Federal samples. However, the asphaltene and maltene fractions are basically two distinct clusters with very limited spread for the asphaltene clusters and the overlap of the maltenes.

The same conclusions based on the six oil samples of this study are also basically true for the three samples of Georgiev *et al.* (2016). The Re-Os isotopic systematics of the asphaltene series of each of the three samples are very similar and cannot determine any geologically meaningful Re-Os dates. Only the maltene fractions of one out of the three oil samples were able to define a Re-Os date that was interpreted as the best estimate of the oil generation age by the authors which is also close to the source rock age.

4.3.4 Implications on the use of asphaltene as substitution of whole oil

The differences of the Re-Os isotopic compositions between the whole oil and its asphaltene depend on the maltene Re and Os contents and the difference of Re-Os isotopic compositions between maltene and asphaltene. More studies are revealing the difference of the Re-Os isotopic compositions between the asphaltenes and their whole oils

and that the maltene fractions account for significant portions of the Re and Os in some oils (Selby *et al.*, 2007; Georgiev *et al.*, 2016; this study). Meanwhile, using the Re and Os more concentrated in the entire asphaltene fraction as substitution of the whole oil for Re-Os geochronology may still be an option in the situation when precise data are required, but cannot be obtain for low Re and Os concentration crude oils. For example, the Unitied Kingdom Atlantic Margin oils (Finlay *et al.*, 2011) and Western Canada Sedimentary Basin Duvernay Formation sourced oils (Liu *et al.*, 2018) have low Re and Os concentrations and thus their asphaltene fractions were analyzed instead for Re-Os isotopic systematics to obtain more precise data. The date defined by the asphaltene Re-Os data corresponds well with the oil generation timing according to Ar-Ar geochronology and basin modeling. Compared to whole oil, utilizing asphaltene can increase the precision of Re-Os data and potentially the Re-Os age.

5 Conclusions

In this study, Re-Os measurements were made on six crude oil samples and their fractions. The crude oils were firstly separated by *n*-heptane into asphaltene and maltene fractions and then the asphaltene fractions were further separated by progressive precipitation using mixtures of dichloromethane and *n*-heptane. The crude oils were also separated into asphaltene and maltene fractions by *n*-pentane, *n*-hexane, *n*-heptane, *n*-octane, *n*-nonane and *n*-decane with dichloromethane and methanol.

Consistent with previous studies, asphaltene fractions are the main carrier of Re and Os in crude oil, no matter if separated solely by *n*-heptane or by *n*-alkane-dichloromethane-methanol solutions. The Re and Os concentration of the fractions of asphaltene decreases throughout the progressive precipitation, with the exception to the first precipitates containing inorganic salts or wax for the Federal, Persian and Viking-Morel oil samples. Throughout the progressive precipitation, both the $^{187}Re/^{188}Os$ and the $^{187}Os/^{188}Os$ values can remain constant, decrease or increase in general for the six samples – no consistent pattern is observed, which means that such properties are dependent on the nature of particular oil, e.g. origin, maturity and alteration. Based on the proposed binding sites of Re and Os in crude oil and the structure of asphaltene, we suggest that the Re and Os in crude oil are to be bound in multiple free compounds, e.g. stable porphyrins and molecules with heteroatomic ligands, and such molecules occluded/absorbed in the asphaltene aggregate structure. Further, we consider that Re and Os can slightly decouple throughout the progressive precipitation and that the radiogenic ^{187}Os can also decouple from the parent ^{187}Re.

Although heterogeneity of $^{187}Re/^{188}Os$ and $^{187}Os/^{188}Os$ between the components of a crude oil is observed by fractionation in this study, no consistent combinations of the fractions of a single crude oil, either from the separation of whole oil by *n*-alkanes or from the progressive precipitation of asphaltene, can consistently yield a geologically meaningful Re-Os age for every one of the six oil samples of this study. Therefore, the extensive use of single oils to obtain meaningful geological dates related to a petroleum system may not be readily viable with the current understanding of the Re-Os systematics of the fractions of crude oil and the currently proposed fractionation

methods. Moreover, in place of whole oil Re-Os analysis for geochronology, utilizing Re-Os data obtained from the whole oil asphaltene fraction may still provide valuable geochronological information of a petroleum system.

Acknowledgements:

This work was supported by both Total and China Scholarship Council awards to Junjie Liu, and the Total Endowment Fund and CUG Wuhan Dida Scholarship to David Selby. The project was also supported by the NERC Innovation award (NE/L008343/1) part of the Oil and Gas Catalyst award scheme. We thank Dr Paul Lillis for providing samples and his constructive comments on the paper; Chris Greenwell for his help on the experiments, and Lloyd R. Snowdon, Zhirong Zhang and Liangbang Ma for their help with the data presentation. We also acknowledge the analytical and mass spectrometry support of Antonia Hofmann, Chris Ottley and Geoff Nowell. We appreciate the constructive comments of Laurie C. Reisberg, Svetoslav Georgiev and another anonymous reviewer that helped to improve this paper.

References

Acevedo, S. c., Guzmán, K., Labrador, H., Carrier, H., Bouyssiere, B., & Lobinski, R. (2012). Trapping of metallic porphyrins by asphaltene aggregates: a size exclusion microchromatography with high-resolution inductively coupled plasma mass spectrometric detection study. *Energy & Fuels, 26*(8), 4968-4977.

Alboudwarej, H., Svrcek, W., Yarranton, H., & Akbarzadeh, K. (2001). *Asphaltene Characterization: Sensitivity of Asphaltene Properties to Extration Techniques*. Paper presented at the Canadian International Petroleum Conference, Calgary, Alberta.

Alsharhan, A., & Nairn, A. (1997). *Sedimentary basins and petroleum geology of the Middle East*. Amsterdam: Elsevier.

Álvarez, E., Trejo, F., Marroquín, G., & Ancheyta, J. (2015). The Effect of Solvent Washing on Asphaltenes and Their Characterization. *Petroleum Science and Technology, 33*(3), 265-271. doi:10.1080/10916466.2014.966918

Barre, A., Prinzhofer, A., & Allegre, C. (1995). Osmium isotopes in the organic matter of crude oil and asphaltenes. *Terra Abs, 7*, 199.

Buckley, J. S. J. E., & Fuels. (1999). Predicting the onset of asphaltene precipitation from refractive index measurements. *13*(2), 328-332.

Buenrostro-Gonzalez, E., Lira-Galeana, C., Gil-Villegas, A., & Wu, J. (2004). Asphaltene precipitation in crude oils: Theory and experiments. *AIChE Journal, 50*(10), 2552-2570. doi:10.1002/aic.10243

Castillo, J., & Vargas, V. (2016). Metal porphyrin occlusion: Adsorption during asphaltene aggregation. *Petroleum Science and Technology, 34*(10), 873-879. doi:10.1080/10916466.2016.1170846

Chacón-Patiño, M. L., Rowland, S. M., & Rodgers, R. P. (2017). Advances in Asphaltene Petroleomics. Part 1: Asphaltenes Are Composed of Abundant Island and Archipelago Structural Motifs. *Energy & Fuels*. doi:10.1021/acs.energyfuels.7b02873

Cheng, B., Zhao, J., Yang, C., Tian, Y., & Liao, Z. (2017). Geochemical Evolution of Occluded Hydrocarbons inside Geomacromolecules: A Review. *Energy & Fuels*. doi:10.1021/acs.energyfuels.7b00454

Clayton, J. L., Warden, A., Daws, T. A., Lillis, P. G., Michael, G. E., & Dawson, M. (1992). *Organic geochemistry of black shales, marlstones, and oils of Middle Pennsylvanian rocks from the northern Denver and southeastern Powder River basins, Wyoming, Nebraska, and Colorado* (1917K). Retrieved from http://pubs.er.usgs.gov/publication/b1917K

Corbett, L. W., & Petrossi, U. (1978). Differences in distillation and solvent separated asphalt residua. *Industrial & Engineering Chemistry Product Research and Development, 17*(4), 342-346.

Cumming, V. M., Selby, D., Lillis, P. G., & Lewan, M. D. (2014). Re–Os geochronology and Os isotope fingerprinting of petroleum sourced from a Type I lacustrine kerogen: Insights from the natural Green River petroleum system in the Uinta Basin and hydrous pyrolysis experiments. *Geochimica et Cosmochimica Acta, 138*, 32-56. doi:10.1016/j.gca.2014.04.016

Derakhshesh, M., Bergmann, A., & Gray, M. R. (2013). Occlusion of Polyaromatic Compounds in Asphaltene Precipitates Suggests Porous Nanoaggregates. *Energy & Fuels, 27*(4), 1748-1751. doi:10.1021/ef3012189

DiMarzio, J. M., Georgiev, S. V., Stein, H. J., & Hannah, J. L. (2018). Residency of rhenium and osmium in a heavy crude oil. *Geochimica et Cosmochimica Acta, 220*, 180-200. doi:10.1016/j.gca.2017.09.038

Durand, E., Clemancey, M., Lancelin, J.-M., Verstraete, J., Espinat, D., & Quoineaud, A.-A. (2010). Effect of Chemical Composition on Asphaltenes Aggregation. *Energy & Fuels, 24*(2), 1051-1062. doi:10.1021/ef900599v

Evdokimov, I. N., Fesan, A. A., & Losev, A. P. (2017). Occlusion of Foreign Molecules in Primary Asphaltene Aggregates from Near-UV–Visible Absorption Studies. *Energy & Fuels, 31*(2), 1370-1375. doi:10.1021/acs.energyfuels.6b02826

Finlay, A. J., Selby, D., & Osborne, M. J. (2011). Re-Os geochronology and fingerprinting of United Kingdom Atlantic margin oil: Temporal implications for regional petroleum systems. *Geology, 39*(5), 475-478. doi:10.1130/G31781.1

Finlay, A. J., Selby, D., & Osborne, M. J. (2012). Petroleum source rock identification of United Kingdom Atlantic Margin oil fields and the Western Canadian Oil Sands using Platinum, Palladium, Osmium and Rhenium: Implications for global petroleum systems. *Earth and Planetary Science Letters, 313-314*, 95-104. doi:10.1016/j.epsl.2011.11.003

Ge, X., Shen, C., Selby, D., Deng, D., & Mei, L. (2016). Apatite fission-track and Re-Os geochronology of the Xuefeng uplift, China: Temporal implications for dry gas associated hydrocarbon systems. *Geology*, G37666. 37661. doi:10.1130/G37666.1

Ge, X., Shen, C., Selby, D., Wang, G., Yang, Z., Gong, Y., & Xiong, S. (2017a). Neoproterozoic-Cambrian petroleum system evolution of the Micang Shan uplift, Northern Sichuan Basin, China: Insights from pyrobitumen Re-Os geochronology and apatite fission track analysis. *AAPG Bulletin*(20,171,108).

Ge, X., Shen, C., Selby, D., Wang, J., Ma, L., Ruan, X., . . . Mei, L. (2017b). Petroleum generation timing and source in the northern Longmen Shan thrust belt, Southwest China: Implications for multiple oil generation episodes and sources. *AAPG Bulletin*(20,170,712).

Georgiev, S. V., Stein, H. J., Hannah, J. L., Galimberti, R., Nali, M., Yang, G., & Zimmerman, A. (2016). Re-Os dating of maltenes and asphaltenes within single samples of crude oil. *Geochimica et Cosmochimica Acta, 179*, 53-75. doi:10.1016/j.gca.2016.01.016

Gramlich, J. W., Murphy, T. J., Garner, E. L., & Shields, W. R. (1973). Absolute isotopic abundance ratio and atomic weight of a reference sample of rhenium. *J. Res. Natl. Bur. Stand. A, 77*, 691-698.

Groenzin, H., Mullins, O. C., Eser, S., Mathews, J., Yang, M.-G., Jones, D. J. E., & Fuels. (2003). Molecular size of asphaltene solubility fractions. *17*(2), 498-503.

Gürgey, K. (1998). Geochemical effects of asphaltene separation procedures: changes in sterane, terpane, and methylalkane distributions in maltenes and asphaltene co-precipitates. *Organic Geochemistry, 29*(5), 1139-1147. doi:http://dx.doi.org/10.1016/S0146-6380(98)00134-X

Isaacs, C. M., & Rullkötter, J. (2001). *The Monterey Formation: From Rocks to Molecules*. New York: Columbia University Press.

James, K. (1990). The Venezuelan hydrocarbon habitat. *Geological Society, London, Special Publications, 50*(1), 9-35.

James, K. (2000). The Venezuelan hydrocarbon habitat, part 1: tectonics, structure, palaeogeography and source rocks. *Journal of Petroleum Geology, 23*(1), 5-53.

Kaminski, T. J., Fogler, H. S., Wolf, N., Wattana, P., & Mairal, A. (2000). Classification of Asphaltenes via Fractionation and the Effect of Heteroatom Content on Dissolution Kinetics. *Energy & Fuels, 14*(1), 25-30. doi:10.1021/ef990111n

Kirschbaum, M., Lillis, P., & Roberts, L. (2007). *Geologic assessment of undiscovered oil and gas resources in the Phosphoria total petroleum system of the Wind River Basin Province, Wyoming* (1411320271). Retrieved from

Liao, Z., Geng, A., Graciaa, A., Creux, P., Chrostowska, A., & Zhang, Y. (2006a). Different Adsorption/Occlusion Properties of Asphaltenes Associated with Their Secondary Evolution Processes in Oil Reservoirs. *Energy & Fuels, 20*(3), 1131-1136. doi:10.1021/ef050355+

Liao, Z., Geng, A., Graciaa, A., Creux, P., Chrostowska, A., & Zhang, Y. (2006b). Saturated hydrocarbons occluded inside asphaltene structures and their geochemical significance, as exemplified by two Venezuelan oils. *Organic Geochemistry, 37*(3), 291-303. doi:10.1016/j.orggeochem.2005.10.010

Liao, Z., Zhao, J., Creux, P., & Yang, C. (2009). Discussion on the Structural Features of Asphaltene Molecules. *Energy & Fuels, 23*(12), 6272-6274. doi:10.1021/ef901126m

Liao, Z., Zhou, H., Graciaa, A., Chrostowska, A., Creux, P., & Geng, A. (2005). Adsorption/Occlusion Characteristics of Asphaltenes: Some Implication for Asphaltene Structural Features. *Energy & Fuels, 19*(1), 180-186. doi:10.1021/ef049868r

Lillis, P. G., & Selby, D. (2013). Evaluation of the rhenium–osmium geochronometer in the Phosphoria petroleum system, Bighorn Basin of Wyoming and Montana, USA. *Geochimica et Cosmochimica Acta, 118*, 312-330. doi:10.1016/j.gca.2013.04.021

Liu, H., Lin, C., Wang, Z., Guo, A., & Chen, K. (2015). Ni, V, and Porphyrinic V Distribution and Its Role in Aggregation of Asphaltenes. *Journal of Dispersion Science and Technology, 36*(8), 1140-1146. doi:10.1080/01932691.2014.961194

Liu, J., & Selby, D. (2018). A Matrix-Matched Reference Material for Validating Petroleum Re-Os Measurements. *Geostandards and Geoanalytical Research, 42*(1), 97-113. doi:10.1111/ggr.12193

Liu, J., Selby, D., Obermajer, M., & Mort, A. (2018). Rhenium–osmium geochronology and oil–source correlation of the Duvernay petroleum system, Western Canada sedimentary basin: Implications for the application of the rhenium–osmium geochronometer to petroleum systems. *AAPG Bulletin, 102*(08), 1627-1657. doi:10.1306/12081717105

Ludwig, K. (2012). *User's manual for Isoplot version 3.75-4.15: A geochronological toolkit for Microsoft Excel* (5 ed.). Berkeley, California: Berkley Geochronological Center.

Mahdaoui, F., Reisberg, L., Michels, R., Hautevelle, Y., Poirier, Y., & Girard, J.-P. (2013). Effect of the progressive precipitation of petroleum asphaltenes on the Re–Os radioisotope system. *Chemical Geology, 358*, 90-100. doi:10.1016/j.chemgeo.2013.08.038

Miller, C. A. (2004). *Re-Os dating of algal laminites reduction-enrichment of metals in the sedimentary environment and evidence for new geoporphyrins.* (Master of Science (M.Sc.)), University of Saskatchewan,

Mitchell, D. L., & Speight, J. G. (1973). The solubility of asphaltenes in hydrocarbon solvents. *Fuel, 52*(2), 149-152.

Mujica, V., Nieto, P., Puerta, L., & Acevedo, S. (2000). Caging of Molecules by Asphaltenes. A Model for Free Radical Preservation in Crude Oils. *Energy & Fuels, 14*(3), 632-639. doi:10.1021/ef990206p

Mullins, O. C. (2010). The Modified Yen Model. *Energy & Fuels, 24*(4), 2179-2207. doi:10.1021/ef900975e

Mullins, O. C., Sabbah, H., Eyssautier, J., Pomerantz, A. E., Barré, L., Andrews, A. B., . . . Zare, R. N. (2012). Advances in Asphaltene Science and the Yen–Mullins Model. *Energy & Fuels, 26*(7), 3986-4003. doi:10.1021/ef300185p

Murgich, J., Abanero, J. A., & Strausz, O. P. (1999). Molecular Recognition in Aggregates Formed by Asphaltene and Resin Molecules from the Athabasca Oil Sand. *Energy & Fuels, 13*(2), 278-286. doi:10.1021/ef980228w

Nalwaya, V., Tantayakom, V., Piumsomboon, P., & Fogler, S. (1999). Studies on Asphaltenes through Analysis of Polar Fractions. *Industrial & Engineering Chemistry Research, 38*(3), 964-972. doi:10.1021/ie9804428

Poplavko, Y., Ivanov, V., Karasik, T., Miller, A., Orekhov, V., Taliyev, S., . . . Fadeyeva, V. (1974). On the concentration of rhenium in petroleum, petroleum bitumens and oil shales. *Geochemistry International, 11*(5), 969-972.

Porte, G., Zhou, H., & Lazzeri, V. J. L. (2003). Reversible description of asphaltene colloidal association and precipitation. *19*(1), 40-47.

Rooney, A. D., Selby, D., Lewan, M. D., Lillis, P. G., & Houzay, J.-P. (2012). Evaluating Re–Os systematics in organic-rich sedimentary rocks in response to petroleum generation using hydrous pyrolysis experiments. *Geochimica et Cosmochimica Acta, 77*, 275-291. doi:10.1016/j.gca.2011.11.006

Selby, D., Creaser, R., Dewing, K., & Fowler, M. (2005). Evaluation of bitumen as a Re–Os geochronometer for hydrocarbon maturation and migration: A test case from the Polaris MVT deposit, Canada. *Earth and Planetary Science Letters, 235*(1-2), 1-15. doi:10.1016/j.epsl.2005.02.018

Selby, D., & Creaser, R. A. (2003). Re–Os geochronology of organic rich sediments: an evaluation of organic matter analysis methods. *Chemical Geology, 200*(3-4), 225-240. doi:10.1016/s0009-2541(03)00199-2

Selby, D., & Creaser, R. A. (2005). Direct radiometric dating of hydrocarbon deposits using rhenium-osmium isotopes. *Science, 308*(5726), 1293-1295. doi:10.1126/science.1111081

Selby, D., Creaser, R. A., & Fowler, M. G. (2007). Re–Os elemental and isotopic systematics in crude oils. *Geochimica et Cosmochimica Acta, 71*(2), 378-386. doi:10.1016/j.gca.2006.09.005

Sheldon, R. P. (1967). Long-distance migration of oil in Wyoming. *The Mountain Geologist, 4*(4), 53-65.

Snowdon, L. R., Volkman, J. K., Zhang, Z., Tao, G., & Liu, P. (2016). The organic geochemistry of asphaltenes and occluded biomarkers. *Organic Geochemistry, 91*, 3-15. doi:http://dx.doi.org/10.1016/j.orggeochem.2015.11.005

Speight, J. (2004). Petroleum Asphaltenes-Part 1: Asphaltenes, resins and the structure of petroleum. *Oil & gas science and technology, 59*(5), 467-477. doi:10.2516/ogst:2004032

Stone, D. S. J. A. B. (1967). Theory of Paleozoic oil and gas accumulation in Big Horn Basin, Wyoming. *American Association of Petroleum Geologists Bulletin, 51*(10), 2056-2114.

Strausz, O. P., Mojelsky, T. W., & Lown, E. M. (1992). The molecular structure of asphaltene: an unfolding story. *Fuel, 71*(12), 1355-1363. doi:https://doi.org/10.1016/0016-2361(92)90206-4

Subramanian, S., Simon, S., & Sjöblom, J. (2016). Asphaltene Precipitation Models: A Review. *Journal of Dispersion Science and Technology, 37*(7), 1027-1049. doi:10.1080/01932691.2015.1065418

Summa, L., Goodman, E., Richardson, M., Norton, I., & Green, A. (2003). Hydrocarbon systems of Northeastern Venezuela: plate through molecular scale-analysis of the genesis and evolution of the Eastern Venezuela Basin. *Marine and Petroleum Geology, 20*(3), 323-349.

Weiss, H., Wilhelms, A., Mills, N., Scotchmer, J., Hall, P., Lind, K., & Brekke, T. (2000). NIGOGA-The Norwegian Industry Guide to Organic Geochemical Analyses. *Norsk Hydro, Statoil, Geolab Nor, SINTEF Petroleum Research and the Norwegian Petroleum Directorate*.

Yarranton, H. W., Ortiz, D. P., Barrera, D. M., Baydak, E. N., Barré, L., Frot, D., . . . Oake, J. (2013). On the Size Distribution of Self-Associated Asphaltenes. *Energy & Fuels, 27*(9), 5083-5106. doi:10.1021/ef400729w

Zhao, X., Liu, Y., Xu, C., Yan, Y., Zhang, Y., Zhang, Q., . . . Shi, Q. (2013). Separation and Characterization of Vanadyl Porphyrins in Venezuela Orinoco Heavy Crude Oil. *Energy & Fuels, 27*(6), 2874-2882. doi:10.1021/ef400161p

Figure 1 scheme of asphaltene progressive precipitation

Figure 2 mass percentages of the progressively precipitated fractions of asphaltenes

Figure 3 mass percentages of the asphaltene and maltene fractions separated by *n*-alkanes from the crude oils

Figure 4 Re-Os concentrations and isotopic ratios of the progressively precipitated fractions of Derby, Federal and Persian asphaltenes

Figure 5 Re-Os concentrations and isotopic ratios of the progressively precipitated fractions of Purisima, RM8505 and Viking-Morel asphaltenes

Figure 6 Re and Os concentrations of asphaltenes separated from all the six crude oil samples with different *n*-alkanes

Figure 7 Re-Os concentrations and isotopic ratios of the maltenes separated from Derby, Federal and Persian samples with different *n*-alkanes

Figure 8 Re-Os concentrations and isotopic ratios of the maltenes separated from Purisima, RM8505 and Viking-Morel samples with different *n*-alkanes

Figure 9 the progressively precipitated asphaltene fractions and the asphaltene and maltene fractions separated by *n*-alkanes of the Derby, Federal and Persian samples in $^{187}Re/^{188}Os$-$^{187}Os/^{188}Os$ space

Figure 10 the progressively precipitated asphaltene fractions and the asphaltene and maltene fractions separated by *n*-alkanes of the Purisima, RM8505 and Viking-Morel samples in $^{187}Re/^{188}Os$-$^{187}Os/^{188}Os$ space

Table 1 Details of the bulk asphaltenes, solvent-precipitant volume and the progressively precipitated fractions of the bulk asphaltenes of the six crude oil samples

Sample	bulk asphaltene percentage	asphaltene used for progressive precipitation (g)	DCM + *n*-C_7 volume (mL)	asphaltene fractions (*n*-C_7: DCM) (g)									sum (g)
				65:35	70:30	75:25	80:20	85:15	90:10	95:5	100:0	soluble	
Derby	5.8%	3.96204	250	NA	0.73968	0.80136	0.48241	0.37525	0.45720	0.20323	0.55605	0.35644	3.97162
Federal	11.9%	1.45679	200	0.18459	0.31873	0.04427	0.12273	0.11901	0.13284	0.09737	0.12285	0.33888	1.48127
Persian	5.7%	4.09564	250	0.22340	0.50225	0.80115	0.65627	0.59451	0.19563	0.48168	0.36309	0.28153	4.09951
Purisima	16.1%	2.22246	200	0.03524	0.36420	0.28343	0.15442	0.35788	0.20701	0.24328	0.25617	0.36664	2.26827
RM8505	13.0%	2.57996	50	NA	1.39920	0.19564	0.20767	0.08468	0.12089	0.05608	0.04785	0.37402	2.48603
Viking-Morel	8.6%	2.64352	200	0.17863	0.42997	0.30998	0.36598	0.21218	0.24913	0.13662	0.23213	0.56725	2.68187

DCM: dichloromethane
NA: not available

Table 2 The separation of crude oils by *n*-alkanes (*n*-C_5, *n*-C_6, *n*-C_7, *n*-C_8, *n*-C_9 and *n*-C_{10}) and DCM-methanol of the six crude oil samples

Alkanes	Oil (g)	Asphalene (g)	Asphaltene (%)	Maltene (g)	Maltene (%)	Asphaltene + maltene	Lost (%)
	Derby oil						
n-C_5	0.99496	0.06312	6.3%	0.75895	76.3%	82.6%	17.4%
n-C_6	0.99726	0.04972	5.0%	0.70854	71.0%	76.0%	24.0%
n-C_7	1.01089	0.05117	5.1%	0.82369	81.5%	86.5%	13.5%
n-C_8	1.12069	0.05545	4.9%	0.91910	82.0%	87.0%	13.0%
n-C_9	1.11289	0.05437	4.9%	0.91384	82.1%	87.0%	13.0%
n-C_{10}	1.01597	0.04958	4.9%	0.85195	83.9%	88.7%	11.3%
	Federal oil						
n-C_5	0.98687	0.10435	10.6%	0.62743	63.6%	74.2%	25.8%
n-C_6	1.00850	0.08491	8.4%	0.79873	79.2%	87.6%	12.4%
n-C_7	0.96435	0.07498	7.8%	0.77333	80.2%	88.0%	12.0%
n-C_8	0.96546	0.07049	7.3%	0.77422	80.2%	87.5%	12.5%
n-C_9	0.96236	0.07123	7.4%	0.77299	80.3%	87.7%	12.3%
n-C_{10}	1.03674	0.07468	7.2%	0.82562	79.6%	86.8%	13.2%

	Persian oil						
n-C_5	0.99286	0.05135	5.2%	0.68212	68.7%	73.9%	26.1%
n-C_6	0.99885	0.04280	4.3%	0.68706	68.8%	73.1%	26.9%
n-C_7	1.00035	0.03586	3.6%	0.69802	69.8%	73.4%	26.6%
n-C_8	1.00058	0.03527	3.5%	0.68989	68.9%	72.5%	27.5%
n-C_9	1.00015	0.03465	3.5%	0.68988	69.0%	72.4%	27.6%
n-C_{10}	0.99429	0.03453	3.5%	0.69784	70.2%	73.7%	26.3%
	Purisima oil						
n-C_5	1.00860	0.12887	12.8%	0.47412	47.0%	59.8%	40.2%
n-C_6	1.01059	0.11445	11.3%	0.52489	51.9%	63.3%	36.7%
n-C_7	1.00100	0.07989	8.0%	0.38971	38.9%	46.9%	53.1%
n-C_8	1.00107	0.08107	8.1%	0.42302	42.3%	50.4%	49.6%
n-C_9	1.03770	0.08064	7.8%	0.45279	43.6%	51.4%	48.6%
n-C_{10}	1.00403	0.10430	10.4%	0.34919	34.8%	45.2%	54.8%
	RM8505						
n-C_5	1.00373	0.09846	9.8%	0.87147	86.8%	96.6%	3.4%
n-C_6	1.19398	0.10209	8.6%	1.04103	87.2%	95.7%	4.3%
n-C_7	0.90893	0.06147	6.8%	0.80135	88.2%	94.9%	5.1%
n-C_8	0.98300	0.08358	8.5%	0.86275	87.8%	96.3%	3.7%
n-C_9	0.97629	0.06405	6.6%	0.85379	87.5%	94.0%	6.0%
n-C_{10}	1.06586	0.08740	8.2%	0.94822	89.0%	97.2%	2.8%
	Viking-Morel oil						
n-C_5	0.99882	0.08070	8.1%	0.72507	72.6%	80.7%	19.3%
n-C_6	1.00929	0.06901	6.8%	0.75534	74.8%	81.7%	18.3%
n-C_7	1.00585	0.06473	6.4%	0.75360	74.9%	81.4%	18.6%
n-C_8	1.01179	0.06374	6.3%	0.75964	75.1%	81.4%	18.6%
n-C_9	1.05958	0.06287	5.9%	0.79222	74.8%	80.7%	19.3%
n-C_{10}	1.00253	0.05951	5.9%	0.75509	75.3%	81.3%	18.7%

Samples are represented by the alkanes used for the separation of asphaltene and maltene

Table 3 Re-Os data synopsis and mass balance for the progressively precipitated asphaltene fractions and the whole oil, *n*-heptane asphaltene and maltene for the Derby oil sample.

Sample [a]	Re (ppb)	u	Os (ppt)	u	^{192}Os (ppt)	u	^{187}Os (ppt)	u	^{187}Re/^{188}Os	u	^{187}Os/^{188}Os	u	rho
70:30	244.6	0.7	2754.1	15.9	832.2	3.5	771.7	3.2	585	3	2.93	0.02	0.61
75:25	219.3	0.6	2404.0	14.4	723.0	3.2	681.9	2.9	603	3	2.99	0.02	0.61
80:20	196.1	0.5	2142.1	12.9	643.5	2.9	609.3	2.7	606	3	3.00	0.02	0.62
85:15	177.7	0.5	1925.5	11.9	578.8	2.7	546.8	2.5	611	3	2.99	0.02	0.63
90:10	145.2	0.4	1609.0	9.5	483.5	2.1	457.3	1.9	597	3	2.99	0.02	0.62
95:5	125.5	0.3	1389.0	8.5	418.8	1.9	391.5	1.7	596	3	2.96	0.02	0.62
100:0	65.4	0.2	773.3	4.6	233.2	1.0	218.0	0.9	558	3	2.96	0.02	0.63
soluble [b]	8.21	0.03	107.5	1.3	32.4	0.6	30.3	0.3	504	9	2.96	0.06	0.82
whole oil	12.16	0.03	144.1	2.0	43.8	0.8	39.9	0.7	553	11	2.88	0.08	0.71
asphaltene	164.4	0.4	1825.7	11.1	548.6	2.5	519.0	2.3	596	3	2.99	0.02	0.63
maltene	1.18	0.01	17.9	0.6	5.4	0.4	5.1	0.2	438	31	3.01	0.24	0.85

u: expanded (k = 2) combined standard uncertainties which include the uncertainties in weighing, blank correction and spike calibrations, mass spectrometry measurements of Re and Os, and the intermediate precision of the results of repeated measurements of Re and Os reference solutions.
rho: error correlation value between 187Re/188Os and 187Os/188Os.
a: the progressively precipitated fractions of asphaltene are represented by the ratio of *n*-heptane to DCM applied in that step.
b: this is the fraction still soluble in the 100% *n*-heptane in the last step of progressive precipitation.

Table 4 Re-Os data synopsis and mass balance for the progressively precipitated asphaltene fractions and the whole oil, *n*-heptane asphaltene and maltene for the Federal oil sample.

Sample [a]	Re (ppb)	u	Os (ppt)	u	^{192}Os (ppt)	u	^{187}Os (ppt)	u	^{187}Re/^{188}Os	u	^{187}Os/^{188}Os	u	rho
65:35	96.2	0.2	567.3	4.1	153.0	0.9	202.8	0.9	1250	8	4.19	0.03	0.71
70:30	84.5	0.4	509.8	4.5	138.0	1.1	181.1	1.2	1218	11	4.15	0.04	0.70
75:25	81.7	0.3	531.5	6.5	147.5	2.3	180.1	1.9	1101	17	3.86	0.07	0.81
80:20	67.2	0.2	449.1	4.2	124.2	1.2	153.3	1.2	1077	10	3.91	0.05	0.75
85:15	67.6	0.3	450.9	8.3	122.3	3.5	159.6	3.3	1100	31	4.13	0.14	0.80
90:10	50.2	0.1	355.0	3.7	98.5	1.1	120.4	1.1	1014	12	3.87	0.06	0.75
95:5	43.1	0.2	319.2	5.5	89.5	2.2	105.9	2.2	958	24	3.75	0.12	0.75
100:0	26.9	0.1	201.2	3.6	53.2	1.4	74.4	1.5	1005	26	4.42	0.15	0.78
soluble [b]	3.19	0.02	30.2	1.4	8.4	0.8	10.2	0.8	755	70	3.83	0.47	0.75
whole oil	8.02	0.03	55.3	1.0	14.9	0.4	19.8	0.4	1071	29	4.22	0.14	0.79
asphaltene	59.5	0.2	386.6	3.1	103.9	0.7	139.0	0.7	1138	8	4.23	0.04	0.74
maltene	1.11	0.01	13.0	0.7	3.7	0.4	4.2	0.3	594	67	3.59	0.50	0.81

u: expanded (k = 2) combined standard uncertainties which include the uncertainties in weighing, blank correction and spike calibrations, mass spectrometry measurements of Re and Os, and the intermediate precision of the results of repeated measurements of Re and Os reference solutions.
rho: error correlation value between 187Re/188Os and 187Os/188Os.
a: the progressively precipitated fractions of asphaltene are represented by the ratio of *n*-heptane to DCM applied in that step.
b: this is the fraction still soluble in the 100% *n*-heptane in the last step of progressive precipitation.

Table 5 Re-Os data synopsis and mass balance for the progressively precipitated asphaltene fractions and the whole oil, *n*-heptane asphaltene and maltene for the Persian oil sample.

Sample [a]	Re (ppb)	u	Os (ppt)	u	^{192}Os (ppt)	u	^{187}Os (ppt)	u	^{187}Re/^{188}Os	u	^{187}Os/^{188}Os	u	rho
65:35	15.9	0.1	55.7	1.3	17.2	0.9	14.7	0.2	1836	90	2.70	0.14	0.98
70:30	79.5	0.2	239.4	1.6	73.3	0.4	64.7	0.3	2156	14	2.79	0.02	0.71
75:25	66.8	0.2	202.3	1.3	61.3	0.3	56.3	0.2	2170	13	2.91	0.02	0.72
80:20	62.4	0.2	195.0	1.4	59.0	0.4	54.4	0.3	2105	15	2.92	0.03	0.75

85:15	48.1	0.1	157.8	1.3	47.2	0.4	45.3	0.3	2026	17	3.03	0.03	0.77
90:10	42.3	0.1	147.2	1.3	43.8	0.4	42.9	0.3	1922	20	3.10	0.04	0.77
95:5	31.3	0.1	124.7	1.2	36.5	0.4	37.8	0.3	1708	20	3.28	0.05	0.77
100:0	12.60	0.03	64.1	0.8	18.6	0.4	19.8	0.2	1347	26	3.36	0.07	0.86
soluble [b]	2.07	0.01	21.2	0.5	6.4	0.3	5.8	0.1	641	29	2.88	0.14	0.94
whole oil	2.83	0.02	11.5	0.4	3.5	0.3	3.0	0.1	1589	136	2.69	0.25	0.90
asphaltene	49.9	0.1	160.6	1.2	48.0	0.4	46.1	0.2	2066	16	3.04	0.03	0.79
maltene	0.34	0.01	4.3	0.4	1.4	0.3	1.0	0.1	488	105	2.21	0.51	0.91

u: expanded (k = 2) combined standard uncertainties which include the uncertainties in weighing, blank correction and spike calibrations, mass spectrometry measurements of Re and Os, and the intermediate precision of the results of repeated measurements of Re and Os reference solutions.
rho: error correlation value between 187Re/188Os and 187Os/188Os.
a: the progressively precipitated fractions of asphaltene are represented by the ratio of *n*-heptane to DCM applied in that step.
b: this is the fraction still soluble in the 100% *n*-heptane in the last step of progressive precipitation.

Table 6 Re-Os data synopsis and mass balance for the progressively precipitated asphaltene fractions and the whole oil, *n*-heptane asphaltene and maltene for the Purisima oil sample.

Sample [a]	Re (ppb)	u	Os (ppt)	u	^{192}Os (ppt)	u	^{187}Os (ppt)	u	^{187}Re/^{188}Os	u	^{187}Os/^{188}Os	u	rho
65:35	119.7	0.4	558.0	3.4	208.2	1.8	62.1	0.4	1144	10	0.95	0.01	0.74
70:30	125.4	0.3	518.1	2.1	192.9	0.8	58.6	0.2	1294	6	0.96	0.01	0.62
75:25	105.1	0.3	397.7	1.8	147.9	0.8	45.4	0.2	1414	9	0.97	0.01	0.69
80:20	92.6	0.2	359.6	1.4	134.6	0.6	38.9	0.2	1369	7	0.92	0.01	0.64
85:15	56.3	0.1	197.3	1.0	73.4	0.5	22.4	0.1	1526	11	0.96	0.01	0.74
90:10	38.3	0.1	130.4	0.8	48.6	0.4	14.6	0.1	1567	14	0.95	0.01	0.83
95:5	42.9	0.1	141.3	5.4	52.4	4.5	16.5	1.3	1630	140	1.00	0.12	0.73
100:0	16.23	0.08	52.6	2.4	19.5	2.0	6.2	0.5	1658	173	1.01	0.13	0.78
soluble [b]	1.39	0.04	6.9	0.9	2.6	0.8	0.7	0.1	1056	328	0.80	0.27	0.92
whole oil	12.09	0.04	41.3	0.5	15.4	0.4	4.6	0.1	1564	38	0.96	0.03	0.80

asphaltene	61.2	0.2	209.6	1.1	77.9	0.5	24.0	0.1	1562	11	0.98	0.01	0.74
maltene	0.59	0.01	6.1	0.3	2.3	0.3	0.52	0.03	502	60	0.71	0.09	0.88

u: expanded (k = 2) combined standard uncertainties which include the uncertainties in weighing, blank correction and spike calibrations, mass spectrometry measurements of Re and Os, and the intermediate precision of the results of repeated measurements of Re and Os reference solutions.
rho: error correlation value between 187Re/188Os and 187Os/188Os.
a: the progressively precipitated fractions of asphaltene are represented by the ratio of *n*-heptane to DCM applied in that step.
b: this is the fraction still soluble in the 100% *n*-heptane in the last step of progressive precipitation.

Table 7 Re-Os data synopsis and mass balance for the progressively precipitated asphaltene fractions and the whole oil, *n*-heptane asphaltene and maltene for the RM8505 oil sample.

Sample [a]	Re (ppb)	u	Os (ppt)	u	^{192}Os (ppt)	u	^{187}Os (ppt)	u	^{187}Re/^{188}Os	u	^{187}Os/^{188}Os	u	rho
70:30	20.73	0.08	197.9	1.8	67.7	0.8	36.6	0.4	609	8	1.71	0.03	0.69
75:25	14.73	0.06	160.4	1.8	55.9	0.9	27.2	0.4	524	9	1.54	0.04	0.70
80:20	11.96	0.05	142.8	1.8	50.2	1.0	23.3	0.5	474	10	1.47	0.04	0.70
85:15	9.90	0.08	126.6	2.7	44.8	1.9	19.8	0.8	439	19	1.40	0.08	0.71
90:10	7.24	0.05	104.2	3.9	37.1	3.0	15.8	1.3	388	32	1.35	0.15	0.71
95:5	5.71	0.11	98.9	3.7	36.1	3.0	13.1	1.0	315	27	1.15	0.13	0.70
100:0	4.07	0.13	81.5	3.2	29.5	2.6	11.3	0.9	275	25	1.21	0.14	0.69
soluble [b]	0.43	0.04	15.2	0.6	5.6	0.5	1.9	0.2	151	19	1.07	0.13	0.55
whole oil	1.88	0.04	23.6	0.9	8.2	0.7	4.0	0.3	454	41	1.54	0.18	0.72
asphaltene	14.56	0.06	147.5	1.9	50.8	1.1	26.4	0.5	570	12	1.65	0.05	0.71
maltene	0.27	0.04	8.2	0.4	3.0	0.4	1.2	0.1	183	35	1.24	0.18	0.54

u: expanded (k = 2) combined standard uncertainties which include the uncertainties in weighing, blank correction and spike calibrations, mass spectrometry measurements of Re and Os, and the intermediate precision of the results of repeated measurements of Re and Os reference solutions.
rho: error correlation value between 187Re/188Os and 187Os/188Os.
a: the progressively precipitated fractions of asphaltene are represented by the ratio of *n*-heptane to DCM applied in that step.
b: this is the fraction still soluble in the 100% *n*-heptane in the last step of progressive precipitation.

Table 8 Re-Os data synopsis and mass balance for the progressively precipitated asphaltene fractions and the whole oil, *n*-heptane asphaltene and maltene for the Viking-Morel oil sample.

Sample [a]	Re (ppb)	u	Os (ppt)	u	^{192}Os (ppt)	u	^{187}Os (ppt)	u	^{187}Re/^{188}Os	u	^{187}Os/^{188}Os	u	rho
65:35	178.8	0.5	2288.7	12.5	686.5	2.5	653.5	2.4	518	2	3.01	0.02	0.58
70:30	201.5	0.5	2575.3	13.9	772.8	2.7	734.5	2.6	519	2	3.01	0.02	0.58
75:25	191.8	0.5	2472.3	13.4	742.5	2.7	703.7	2.5	514	2	3.00	0.02	0.58
80:20	167.7	0.4	2207.5	12.2	663.3	2.5	627.4	2.4	503	2	2.99	0.02	0.59
85:15	147.2	0.4	1999.1	11.3	600.9	2.4	567.7	2.2	487	2	2.99	0.02	0.60
90:10	122.3	0.3	1743.9	10.4	524.5	2.3	494.4	2.1	464	2	2.98	0.02	0.62
95:5	100.2	0.3	1477.7	9.9	443.9	2.4	420.3	2.2	449	3	3.00	0.02	0.64
100:0	63.9	0.2	997.6	8.8	301.5	2.6	279.5	2.4	422	4	2.93	0.04	0.68
soluble [b]	8.91	0.03	153.5	1.5	46.1	0.5	43.7	0.4	385	4	3.01	0.04	0.74
whole oil	12.33	0.03	173.3	2.3	52.1	0.9	49.1	0.8	471	8	2.98	0.07	0.71
asphaltene	129.9	0.3	1736.8	9.6	521.0	1.9	495.8	1.8	496	2	3.01	0.02	0.58
maltene	1.57	0.01	31.2	0.8	9.5	0.5	8.6	0.3	330	17	2.85	0.18	0.76

u: expanded (k = 2) combined standard uncertainties which include the uncertainties in weighing, blank correction and spike calibrations, mass spectrometry measurements of Re and Os, and the intermediate precision of the results of repeated measurements of Re and Os reference solutions.
rho: error correlation value between 187Re/188Os and 187Os/188Os.
a: the progressively precipitated fractions of asphaltene are represented by the ratio of *n*-heptane to DCM applied in that step.
b: this is the fraction still soluble in the 100% *n*-heptane in the last step of progressive precipitation.

Table 9 the recovered Re and Os in concentrations and percentages and expected isotopic ratios of the progressive precipitation of asphaltenes

Sample	mass (%) [a]	Re (ppb) [b]	^{192}Os (ppt) [b]	^{187}Os (ppt) [b]	Re [c]	^{192}Os [c]	^{187}Os [c]	^{187}Re/^{188}Os [d]	^{187}Re/^{188}Os i [e]	^{187}Os/^{188}Os [d]	^{187}Os/^{188}Os i [e]
Derby	100.2	163.8	547.7	514.1	100%	100%	99%	595	596	2.97	2.99
Federal	101.7	54.8	95.9	123.4	92%	92%	89%	1137	1138	4.07	4.23
Persian	100.1	47.6	46.7	43.7	95%	97%	95%	2029	2066	2.96	3.04
Purisima	102.1	61.7	87.9	26.7	101%	113%	111%	1397	1562	0.96	0.98
RM8505	96.4	14.2	50.4	26.0	98%	99%	98%	563	570	1.63	1.65
Viking-Morel	101.5	126.6	508.0	480.8	97%	97%	97%	496	496	3.00	3.01

a: recovery of the mass of the fractions, the ratio of the total mass of all the fractions to the original bulk asphaltene used;
b: recovered concentrations of Re, common Os (represented by ^{192}Os) and ^{187}Os; the total of Re (, ^{192}Os and ^{187}Os) concentrations of each fraction multiply by their mass percentages of the original bulk asphaltenes
c: recovered concentrations of Re, common Os (represented by ^{192}Os) and ^{187}Os divided by the concentrations of the original bulk asphaltenes;
d: expected bulk asphaltene isotopic ratios from the Re-Os measurements of all the fractions;
e: measured bulk asphaltene isotopic ratios.

Table 10 Re-Os data synopsis for the asphaltene fractions separated by *n*-alkane-DCM-methanol from the six oil samples

Sample	Re (ppb)	±	Os (ppt)	±	^{192}Os (ppt)	±	^{187}Os (ppt)	±	^{187}Re/^{188}Os	±	^{187}Os/^{188}Os	±	rho
Derby oil													
n-C_5	152.7	0.4	1709.0	10.2	514.3	2.3	483.8	2.1	590	3	2.98	0.02	0.61
n-C_6	154.9	0.4	1745.1	10.7	525.5	2.5	493.3	2.2	586	3	2.97	0.02	0.63
n-C_7	169.4	0.6	1820.0	11.2	548.0	2.6	514.8	2.3	615	4	2.97	0.02	0.59
n-C_8	168.0	0.5	1860.7	11.4	560.0	2.6	526.8	2.4	597	3	2.98	0.02	0.62
n-C_9	168.8	0.5	1822.0	11.2	548.5	2.6	515.5	2.3	612	3	2.97	0.02	0.63
n-C_{10}	166.0	0.5	1786.4	11.0	537.9	2.6	505.2	2.3	614	3	2.97	0.02	0.62
Federal													

oil													
n-C_5	66.5	0.2	395.2	3.2	106.9	0.7	140.7	0.8	1238	9	4.17	0.04	0.68
n-C_6	74.1	0.2	440.7	3.7	119.2	0.9	156.7	1.0	1236	10	4.16	0.04	0.72
n-C_7	73.3	0.2	450.2	4.0	121.9	1.0	160.0	1.1	1196	10	4.15	0.04	0.73
n-C_8	77.9	0.2	455.5	4.0	123.5	1.0	161.3	1.1	1255	11	4.13	0.04	0.72
n-C_9	75.4	0.2	443.6	3.9	120.2	1.0	157.4	1.1	1249	11	4.15	0.04	0.74
n-C_{10}	72.8	0.2	442.3	3.9	119.9	1.0	156.7	1.1	1209	10	4.14	0.04	0.73
Persian oil													
n-C_5	51.1	0.1	163.7	2.0	49.4	0.9	46.0	0.4	2058	38	2.94	0.06	0.89
n-C_6	57.8	0.2	181.2	2.2	55.0	1.1	50.3	0.4	2090	41	2.89	0.06	0.90
n-C_7	60.1	0.2	197.5	2.5	60.2	1.3	54.2	0.5	1989	41	2.85	0.06	0.91
n-C_8	64.4	0.2	206.7	2.9	63.5	1.6	55.3	0.5	2018	50	2.76	0.07	0.93
n-C_9	64.4	0.2	200.1	2.6	60.9	1.3	55.1	0.5	2103	45	2.86	0.07	0.91
n-C_{10}	63.9	0.2	200.4	2.6	61.3	1.3	54.4	0.5	2075	44	2.81	0.06	0.91
Purisima oil													
n-C_5	70.2	0.2	253.7	1.2	94.3	0.6	29.0	0.1	1480	9	0.97	0.01	0.70
n-C_6	75.7	0.2	291.0	1.4	108.2	0.6	33.2	0.2	1392	9	0.97	0.01	0.70
n-C_7	79.5	0.2	308.2	1.6	114.7	0.8	35.0	0.2	1378	10	0.97	0.01	0.74
n-C_8	84.3	0.2	321.2	1.7	119.6	0.8	36.4	0.2	1402	10	0.96	0.01	0.72
n-C_9	95.7	0.5	333.7	1.7	124.2	0.8	37.9	0.2	1533	13	0.97	0.01	0.60
n-C_{10}	76.2	0.2	296.6	2.6	110.5	1.6	33.4	0.4	1372	20	0.96	0.02	0.78
RM8505													
n-C_5	19.4	0.1	189.4	1.9	65.8	1.0	32.7	0.5	586	9	1.57	0.03	0.73
n-C_6	20.4	0.1	197.3	2.0	68.4	1.0	34.4	0.5	593	9	1.59	0.03	0.72
n-C_7	23.3	0.1	216.6	2.3	74.9	1.2	38.1	0.5	619	10	1.61	0.03	0.75
n-C_8	18.8	0.1	174.0	1.9	60.1	1.0	31.0	0.5	622	11	1.63	0.04	0.72
n-C_9	23.0	0.	213.2	2.3	73.8	1.	37.4	0.	619	1	1.61	0.0	0.7

		1				2		5		0		3	5
n-C_{10}	18.8	0.1	177.7	1.9	61.4	1.0	31.3	0.4	608	10	1.61	0.03	0.74
Viking-Morel oil													
n-C_5	143.9	0.5	1825.5	10.8	548.3	2.4	519.4	2.2	522	3	3.00	0.02	0.55
n-C_6	153.9	0.4	1916.6	11.6	575.5	2.6	545.9	2.4	532	3	3.00	0.02	0.60
n-C_7	158.0	0.5	1896.0	11.5	569.4	2.6	539.7	2.4	552	3	3.00	0.02	0.58
n-C_8	152.7	0.5	1891.6	11.5	568.2	2.6	538.2	2.4	535	3	3.00	0.02	0.60
n-C_9	159.0	0.6	1875.1	11.4	563.1	2.6	533.7	2.4	562	3	3.00	0.02	0.57
n-C_{10}	153.0	1.1	1858.4	11.4	558.3	2.6	528.4	2.4	545	5	3.00	0.02	0.38

Samples are represented by the alkanes used for the separation of asphaltene and maltene

Table 11 Re-Os data synopsis for the maltene fractions separated by *n*-alkane-DCM-methanol from the six oil samples

Sample	**Re (ppb)**	**±**	**Os (ppt)**	**±**	**^{192}Os (ppt)**	**±**	**^{187}Os (ppt)**	**±**	**^{187}Re/^{188}Os**	**±**	**^{187}Os/^{188}Os**	**±**	**rho**
Derby oil													
n-C_5	1.81	0.01	27.9	1.2	8.8	0.8	7.0	0.6	410	36	2.54	0.30	0.73
n-C_6	2.61	0.01	36.6	1.5	11.4	1.0	9.5	0.8	457	39	2.64	0.31	0.73
n-C_7	3.42	0.03	46.1	2.0	14.3	1.2	12.1	1.0	476	41	2.68	0.32	0.73
n-C_8	3.79	0.02	48.7	2.0	15.1	1.3	12.7	1.0	499	42	2.67	0.31	0.72
n-C_9	3.63	0.02	47.9	2.0	14.8	1.2	12.6	1.0	488	41	2.70	0.31	0.72
n-C_{10}	3.71	0.02	47.8	2.0	14.7	1.2	12.7	1.0	502	42	2.74	0.32	0.72
Federal oil													
n-C_5	1.33	0.01	15.6	0.8	4.6	0.5	4.6	0.4	576	61	3.20	0.43	0.79
n-C_6	2.10	0.02	20.6	1.0	5.8	0.6	6.7	0.5	716	71	3.62	0.46	0.77
n-C_7	2.55	0.02	22.5	1.1	6.3	0.6	7.4	0.6	803	76	3.73	0.46	0.76
n-C_8	3.04	0.02	28.2	1.3	8.1	0.7	8.9	0.7	743	67	3.46	0.42	0.74

n-C_9	3.01	0.02	26.5	1.2	7.5	0.7	8.6	0.7	795	72	3.60	0.44	0.74
n-C_{10}	3.20	0.02	28.2	1.3	8.0	0.7	9.2	0.7	799	72	3.64	0.44	0.74
Persian oil													
n-C_5	0.57	0.01	4.7	0.4	1.5	0.3	1.1	0.1	746	155	2.22	0.49	0.92
n-C_6	0.86	0.01	5.5	0.4	1.8	0.3	1.3	0.1	967	170	2.32	0.45	0.90
n-C_7	1.20	0.01	6.6	0.4	2.0	0.3	1.7	0.1	1168	185	2.60	0.46	0.88
n-C_8	1.22	0.01	6.5	0.4	2.0	0.3	1.7	0.1	1203	190	2.63	0.47	0.88
n-C_9	1.25	0.01	7.3	0.4	2.3	0.3	1.9	0.2	1092	163	2.60	0.44	0.87
n-C_{10}	1.45	0.01	7.1	0.4	2.2	0.3	1.8	0.2	1322	204	2.67	0.47	0.88
Purisima oil													
n-C_5	0.70	0.01	7.7	0.4	3.0	0.4	0.4	0.0	456	58	0.47	0.08	0.77
n-C_6	1.13	0.01	7.1	0.4	2.8	0.4	0.6	0.1	812	109	0.63	0.10	0.81
n-C_7	1.40	0.01	8.2	0.4	3.2	0.4	0.7	0.1	880	108	0.65	0.10	0.80
n-C_8	1.48	0.01	8.5	0.4	3.3	0.4	0.7	0.1	902	108	0.68	0.10	0.79
n-C_9	1.83	0.01	10.0	0.5	3.9	0.4	0.8	0.1	943	106	0.69	0.10	0.79
n-C_{10}	1.31	0.02	7.5	0.4	2.9	0.4	0.6	0.1	904	124	0.66	0.11	0.82
RM8505													
n-C_5	0.75	0.01	12.2	0.5	4.5	0.5	1.5	0.1	331	34	1.05	0.14	0.77
n-C_6	0.58	0.01	12.9	0.6	4.7	0.5	1.7	0.1	244	25	1.17	0.15	0.76
n-C_7	0.81	0.02	15.8	0.7	5.7	0.6	2.2	0.2	281	30	1.22	0.16	0.77
n-C_8	0.92	0.02	16.6	0.8	6.0	0.6	2.3	0.2	307	33	1.23	0.16	0.77
n-C_9	1.20	0.02	17.1	0.8	6.2	0.6	2.4	0.2	387	40	1.22	0.16	0.77
n-C_{10}	1.39	0.02	17.3	0.8	6.2	0.6	2.5	0.2	445	45	1.25	0.16	0.77
Viking-Morel oil													
n-C_5	2.04	0.02	37.3	1.6	11.4	1.0	10.2	0.8	356	31	2.83	0.33	0.73
n-C_6	3.24	0.02	60.7	2.6	18.5	1.5	16.5	1.3	348	29	2.82	0.33	0.71
n-C_7	4.39	0.0	70.8	3.	21.4	1.	19.7	1.	408	34	2.92	0.3	0.7

		2		0		8		6				4	1
n-C_8	4.63	0.02	73.3	3.1	22.4	1.8	19.9	1.6	411	34	2.82	0.32	0.71
n-C_9	5.35	0.02	84.3	3.5	25.6	2.1	23.3	1.9	416	34	2.88	0.33	0.71
n-C_{10}	5.82	0.03	95.2	4.0	28.9	2.4	26.2	2.1	400	33	2.87	0.33	0.71

Samples are represented by the alkanes used for the separation of asphaltene and maltene

Table 12 Geochronology of the fractions of asphaltenes of the six crude oil samples in this study

Sample	**source rock**	**oil generation**	**asphaltene fractions by progressive precipitation (n = 8 or 9)**	**selection of asphaltene fractions**
Derby	Permian Phosphoria Formation	since Late Triassic and before Laramide orogeny	Isoplot Model III, 26 ± 43 Ma (Os_i = 2.71 ± 0.42, MSWD = 5.3)	70:30, 75:25, 80:20, 95:5; Model I, 170 ± 50 Ma (Os_i = 1.27 ± 0.50, MSWD = 0.5)
Federal	Permian Phosphoria Formation	since Late Triassic and before Laramide orogeny	Isoplot Model III, 43 ± 82 Ma (Os_i = 3.3 ± 1.5, MSWD = 18)	excluding 85:15, 100:0 and soluble; Model III, 91 ± 35 Ma (Os_i = 2.28 ± 0.65, MSWD = 4.5)
Persian	Cretaceous and/or Late Jurassic	unknown	Isoplot Model III, -6 ± 23 Ma (Os_i = 3.17 ± 0.72, MSWD = 36)	/
Purisima	Miocene Monterey Formation	in the last five million years	Isoplot Model III, 2.8 ± 7.7 Ma (Os_i = 0.89 ± 0.18, MSWD = 32)	65:35, 70:30, 75:25; Model I, 5.5 ± 2.5 Ma (Os_i = 0.84 ± 0.06, MSWD = 0.4)
RM8505	Upper Cretaceous La Luna Formation (Presumably)	since Miocene	Isoplot Model I, 98.4 ± 9.5 Ma (Osi = 0.70 ± 0.09, MSWD = 1.9)	/
Viking-Morel	Pennsylvanian-Permian Minnelusa Formation	unkown	Isoplot Model III, 17 ± 11 Ma (Os_i = 2.9 ± 0.1, MSWD = 2)	/

Table 13 Geochronology of the asphaltene and maltene fractions of the six crude oil samples in this study

Sample	source rock	oil generation	asphaltene and maltene (*n*-heptane), crude oil	Asphaltenes separated by *n*-alkanes (n = 6)	Maltenes separated by *n*-alkanes (n = 6)	Asphaltenes and maltenes separated by *n*-alkanes plus crude oil (n = 13)
Derby	Permian Phosphoria Formation	since Late Triassic before Laramide orogeny	Isoplot Model III, -5 ± 790 Ma (Os_i = 3.0 ± 7.4, MSWD = 6.0)	Isoplot Model I, -3 ± 39 Ma (Os_i = 3.00 ± 0.39, MSWD = 0.09)	Isoplot Model I, 110 ± 200 Ma (Os_i = 1.8 ± 1.6, MSWD = 0.04)	Isoplot Model III, 96 ± 43 Ma (Os_i = 2.00 ± 0.43, MSWD = 2.1)
Federal	Permian Phosphoria Formation	since Late Triassic before Laramide orogeny	Isoplot Model I, 61 ± 44 Ma (Os_i = 3.07 ± 0.83, MSWD = 0.86)	Isoplot Model I, -6 ± 50 Ma (Os_i = 4.3 ± 1.0, MSWD = 0.55)	Isoplot Model I, 113 ± 110 Ma (Os_i = 2.1 ± 1.3, MSWD = 0.25)	Isoplot Model III, 67 ± 22 Ma (Os_i = 2.80 ± 0.44, MSWD = 2.5)
Persian	Cretaceous and/or Late Jurassic	unknown	Isoplot Model I, 35 ± 14 Ma (Os_i = 1.82 ± 0.48, MSWD = 0.71)	Isoplot Model III, 18 ± 120 Ma (Os_i = 2.2 ± 4.1, MSWD = 3.5)	Isoplot Model I, 51 ± 46 Ma (Os_i = 1.59 ± 0.85, MSWD = 0.16)	Isoplot Model III, 21 ± 11 Ma (Os_i = 2.12 ± 0.37, MSWD = 2.6)
Purisima	Miocene Monterey Formation	in the last five million years	Isoplot Model I, 14.4 ± 4.5 Ma (Os_i = 0.60 ± 0.12, MSWD = 3.5)	Isoplot Model I, 0.4 ± 3.4 Ma (Os_i = 0.96 ± 0.08, MSWD = 1.4)	Isoplot Model I, 27.3 ± 8.7 Ma (Osi = 0.26 ± 0.12, MSWD = 0.07)	Isoplot Model III, 30.1 ± 4.3 Ma (Os_i = 0.24 ± 0.09, MSWD = 24)
RM8505	Upper Cretaceous La Luna Formation (Presumably)	since Miocene	Isoplot Model I, 62 ± 25 Ma (Os_i = 1.06 ± 0.23, MSWD = 0.03)	Isoplot Model I, 65 ± 47 Ma (Os_i = 0.94 ± 0.47, MSWD = 0.64)	Isoplot Model I, 6 ± 58 Ma (Os_i = 1.15 ± 0.33, MSWD = 1.3)	Isoplot Model III, 83 ± 20 Ma (Os_i = 0.76 ± 0.18, MSWD = 2.3)
Viking-Morel	Pennsylvanian-Permian Minnelusa Formation	unkown	Isoplot Model I, 59 ± 57 Ma (Os_i = 2.52 ± 0.47, MSWD = 0.02)	Isoplot Model I, 0 ± 34 Ma (Os_i = 3.00 ± 0.30, MSWD = 0.08)	Isoplot Model I, 40 ± 280 Ma (Os_i = 2.6 ± 1.8, MSWD = 0.06)	Isoplot Model I, 16 ± 25 Ma (Os_i = 2.86 ± 0.22, MSWD = 0.36)

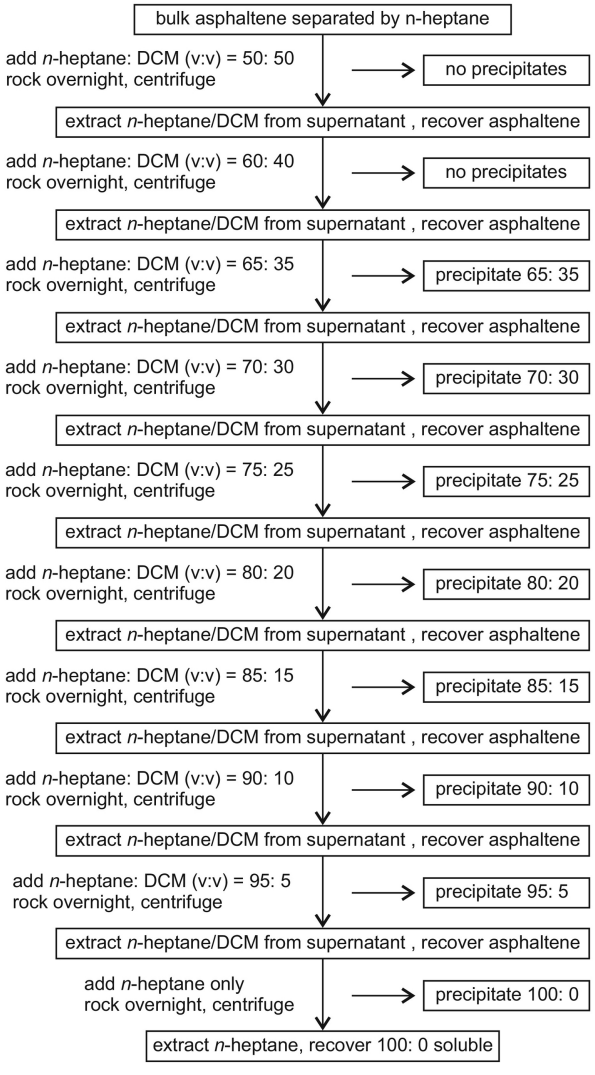
bulk asphaltene separated by n-heptane
add n-heptane: DCM (v:v) = 50: 50
rock overnight, centrifuge
no precipitates
extract n-heptane/DCM from supernatant , recover asphaltene
add n-heptane: DCM (v:v) = 60: 40
rock overnight, centrifuge
no precipitates
extract n-heptane/DCM from supernatant , recover asphaltene
add n-heptane: DCM (v:v) = 65: 35
rock overnight, centrifuge
precipitate 65: 35
extract n-heptane/DCM from supernatant , recover asphaltene
add n-heptane: DCM (v:v) = 70: 30
rock overnight, centrifuge
precipitate 70: 30
extract n-heptane/DCM from supernatant , recover asphaltene
add n-heptane: DCM (v:v) = 75: 25
rock overnight, centrifuge
precipitate 75: 25
extract n-heptane/DCM from supernatant , recover asphaltene
add n-heptane: DCM (v:v) = 80: 20
rock overnight, centrifuge
precipitate 80: 20
extract n-heptane/DCM from supernatant , recover asphaltene
add n-heptane: DCM (v:v) = 85: 15
rock overnight, centrifuge
precipitate 85: 15
extract n-heptane/DCM from supernatant , recover asphaltene
add n-heptane: DCM (v:v) = 90: 10
rock overnight, centrifuge
precipitate 90: 10
extract n-heptane/DCM from supernatant , recover asphaltene
add n-heptane: DCM (v:v) = 95: 5
rock overnight, centrifuge
precipitate 95: 5
extract n-heptane/DCM from supernatant , recover asphaltene
add n-heptane only
rock overnight, centrifuge
precipitate 100: 0
extract n-heptane, recover 100: 0 soluble

Figure 1

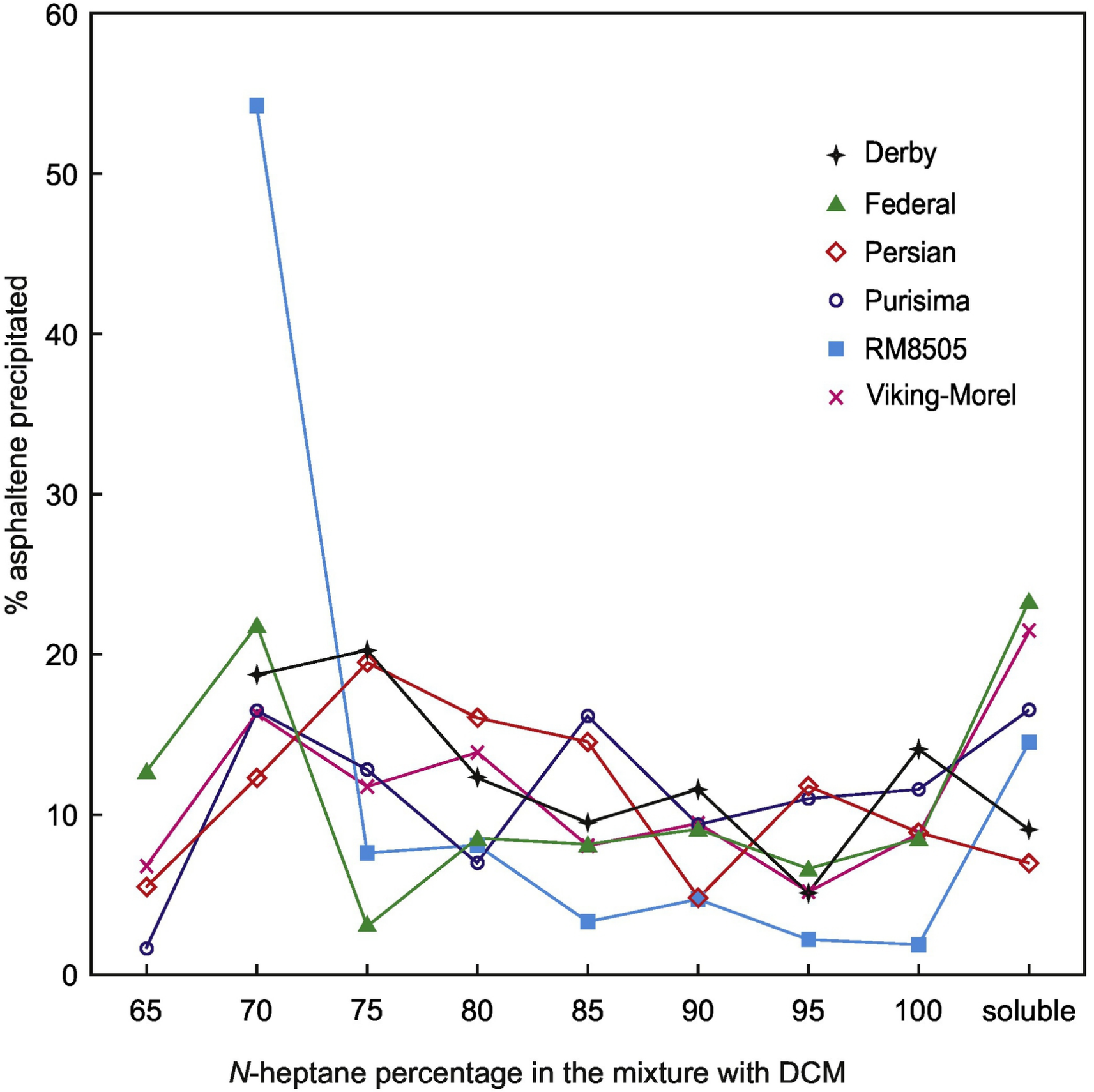
60
50
40
30
20
10
0
% asphaltene precipitated
Derby
Federal
Persian
Purisima
RM8505
Viking-Morel
65
70
75
80
85
90
95
100
soluble
N-heptane percentage in the mixture with DCM

Figure 2

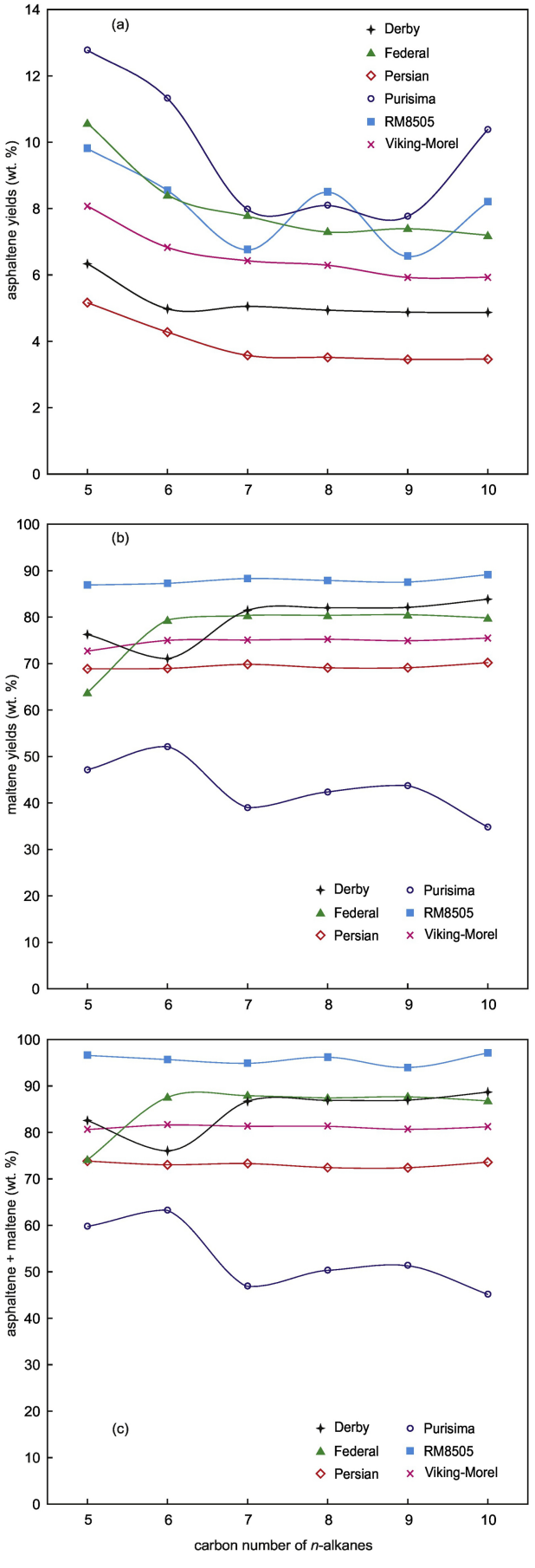
(a)
Derby
Federal
Persian
Purisima
RM8505
Viking-Morel
asphaltene yields (wt. %)
(b)
maltene yields (wt. %)
(c)
asphaltene + maltene (wt. %)
carbon number of n-alkanes

Figure 3

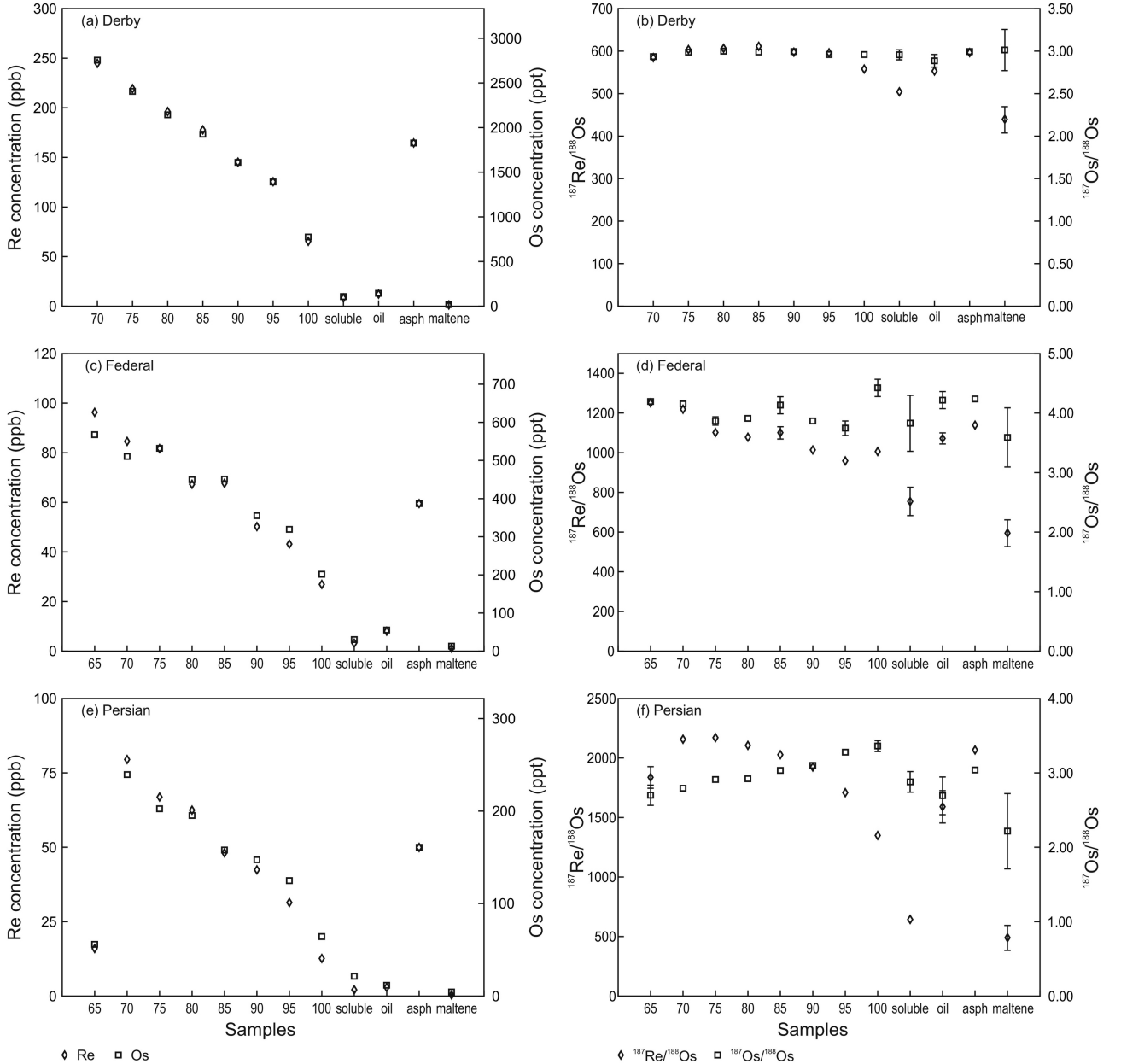
(a) Derby
Re concentration (ppb)
Os concentration (ppt)
(b) Derby
$^{187}Re/^{188}Os$
$^{187}Os/^{188}Os$
(c) Federal
(d) Federal
(e) Persian
(f) Persian
70 75 80 85 90 95 100 soluble oil asph maltene
65 70 75 80 85 90 95 100 soluble oil asph maltene
Samples
Re Os
$^{187}Re/^{188}Os$ $^{187}Os/^{188}Os$

Figure 4

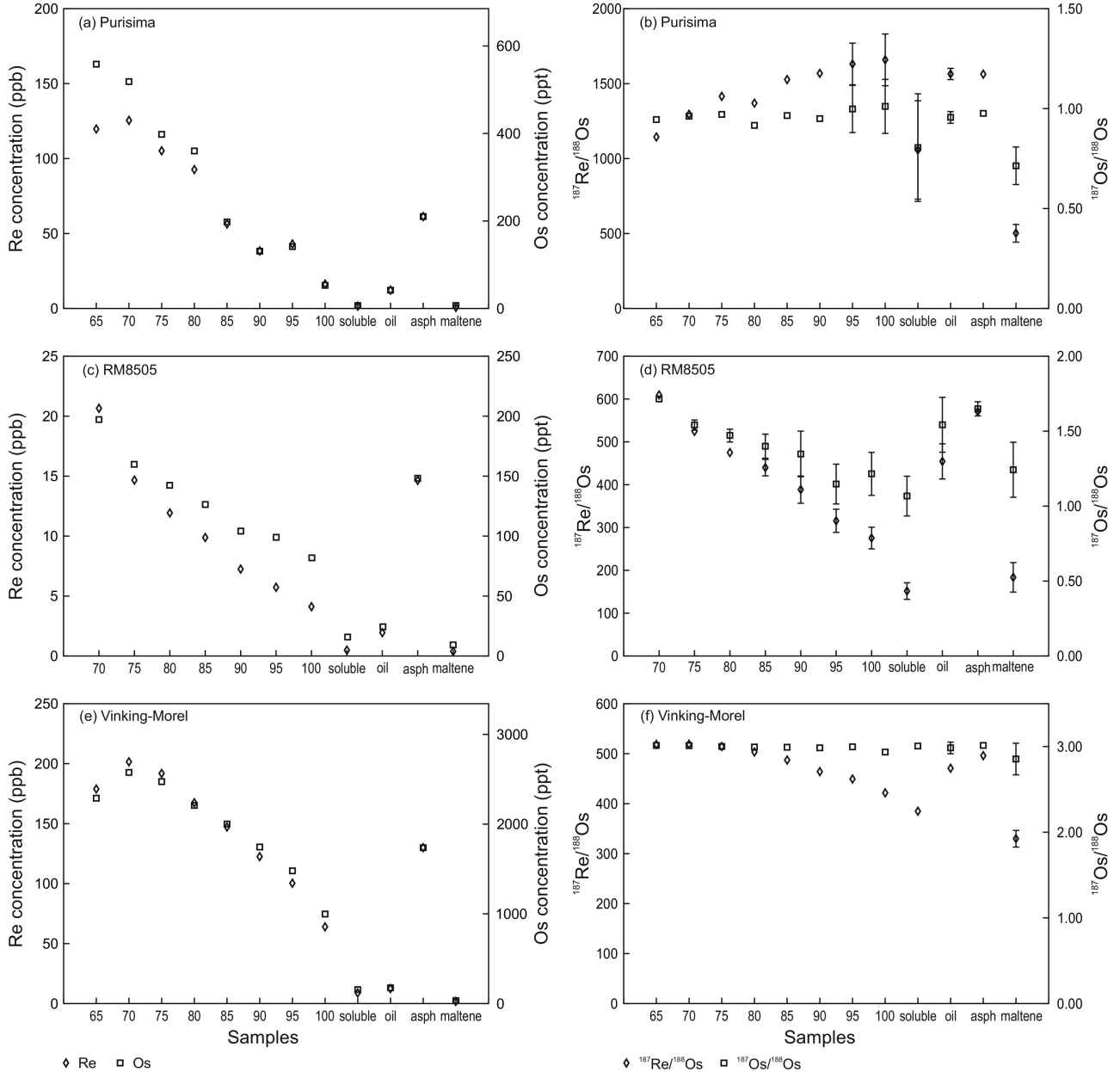
(a) Purisima
(b) Purisima
(c) RM8505
(d) RM8505
(e) Vinking-Morel
(f) Vinking-Morel
Re concentration (ppb)
Os concentration (ppt)
$^{187}Re/^{188}Os$
$^{187}Os/^{188}Os$
65 70 75 80 85 90 95 100 soluble oil asph maltene
Samples
Re
Os
$^{187}Re/^{188}Os$
$^{187}Os/^{188}Os$

Figure 5

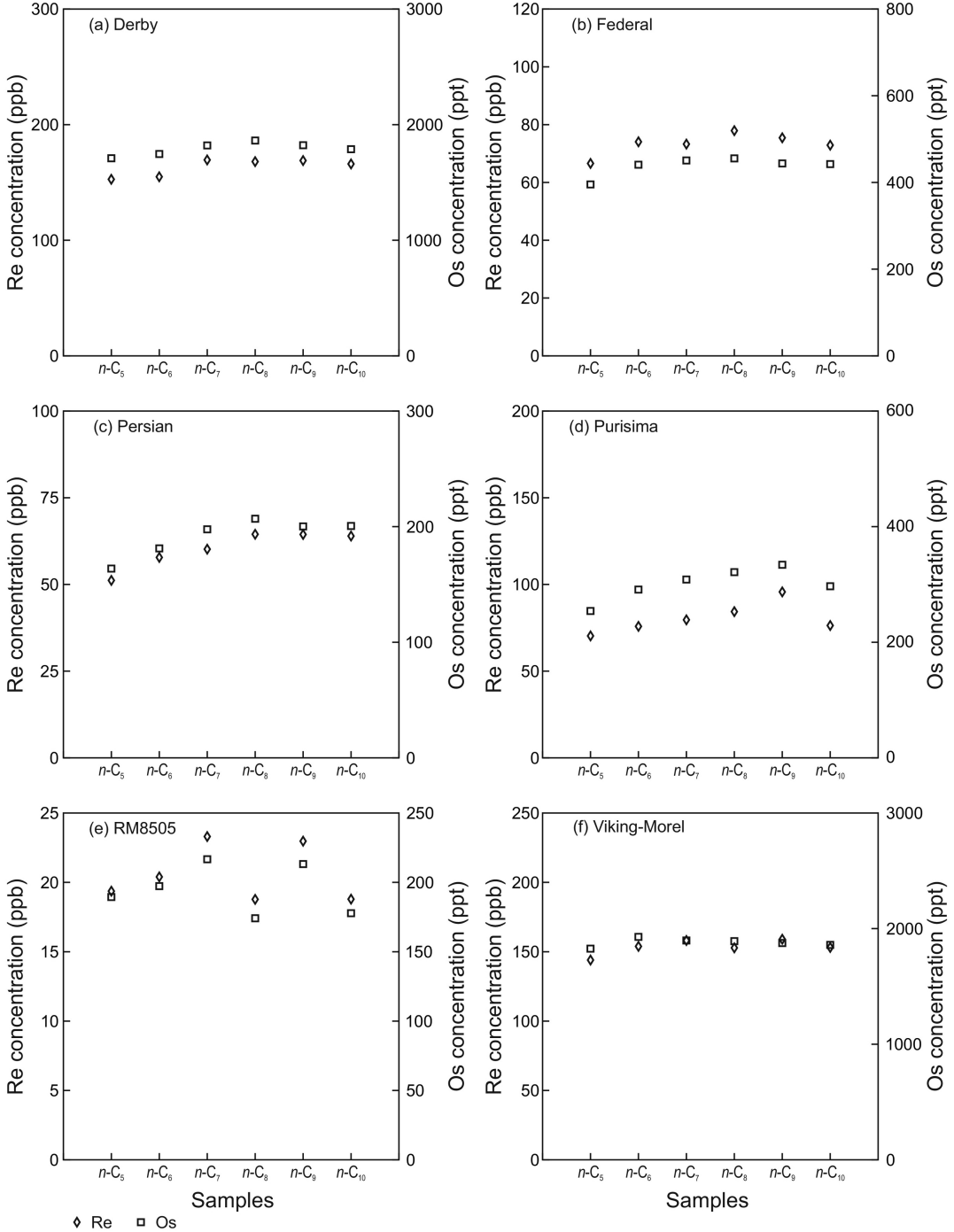
(a) Derby
(b) Federal
(c) Persian
(d) Purisima
(e) RM8505
(f) Viking-Morel
Re concentration (ppb)
Os concentration (ppt)
n-C5
n-C6
n-C7
n-C8
n-C9
n-C10
Samples
Re
Os

Figure 6

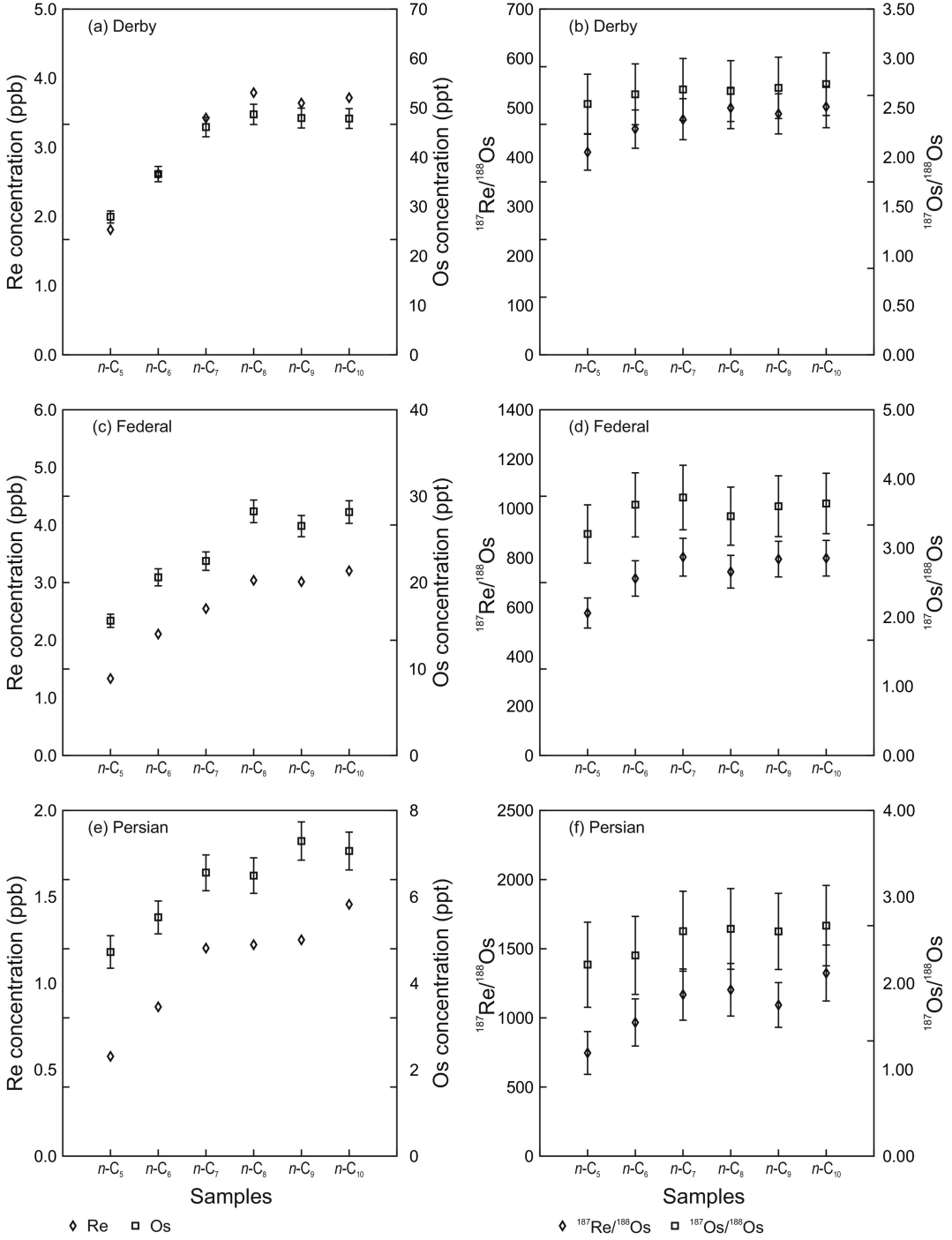
(a) Derby
(b) Derby
(c) Federal
(d) Federal
(e) Persian
(f) Persian
Re concentration (ppb)
Os concentration (ppt)
$^{187}Re/^{188}Os$
$^{187}Os/^{188}Os$
n-C5
n-C6
n-C7
n-C8
n-C9
n-C10
Samples
Re
Os

Figure 7

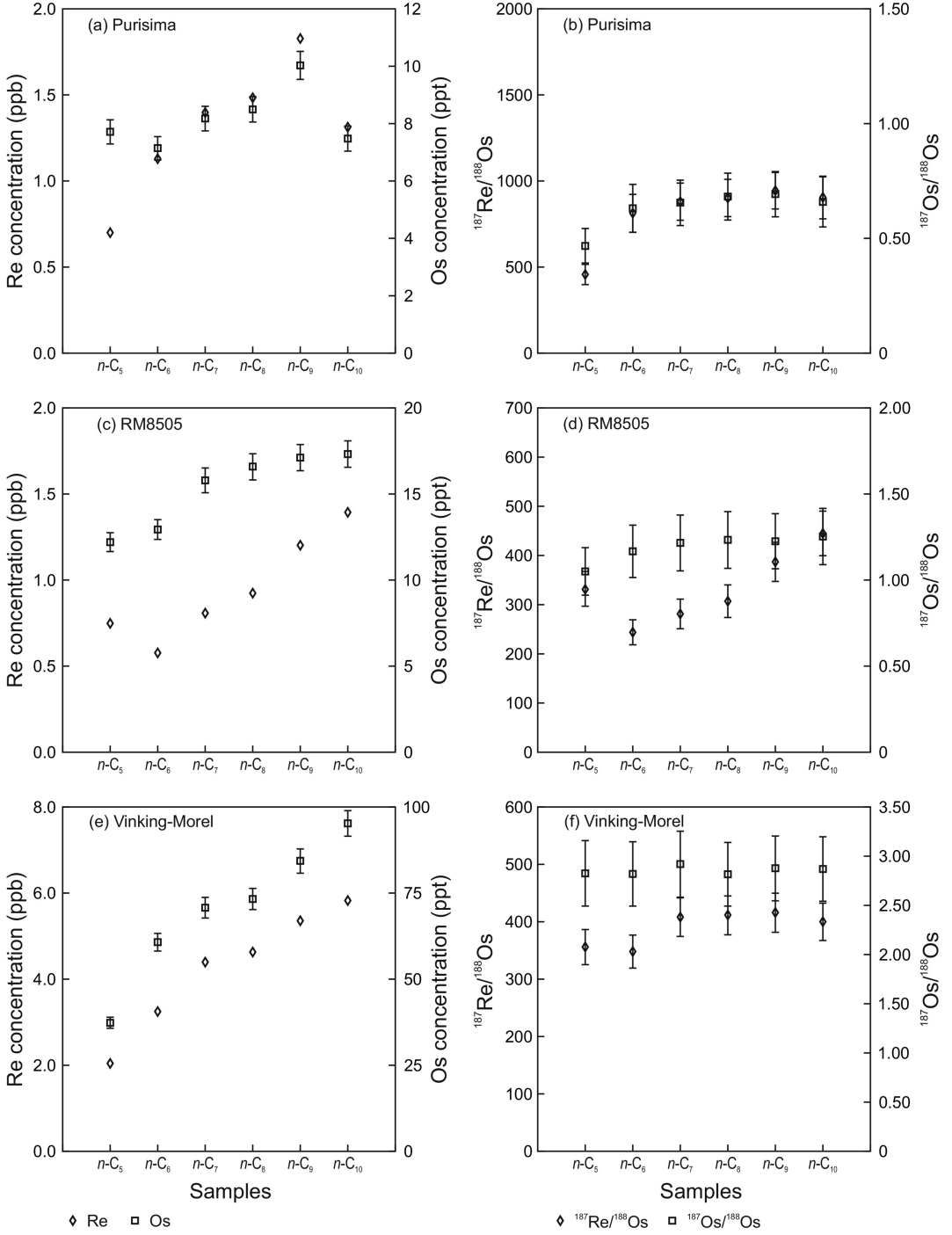
(a) Purisima
(b) Purisima
(c) RM8505
(d) RM8505
(e) Vinking-Morel
(f) Vinking-Morel
Re concentration (ppb)
Os concentration (ppt)
$^{187}Re/^{188}Os$
$^{187}Os/^{188}Os$
n-C5
n-C6
n-C7
n-C8
n-C9
n-C10
Samples
Re
Os
$^{187}Re/^{188}Os$
$^{187}Os/^{188}Os$

Figure 8

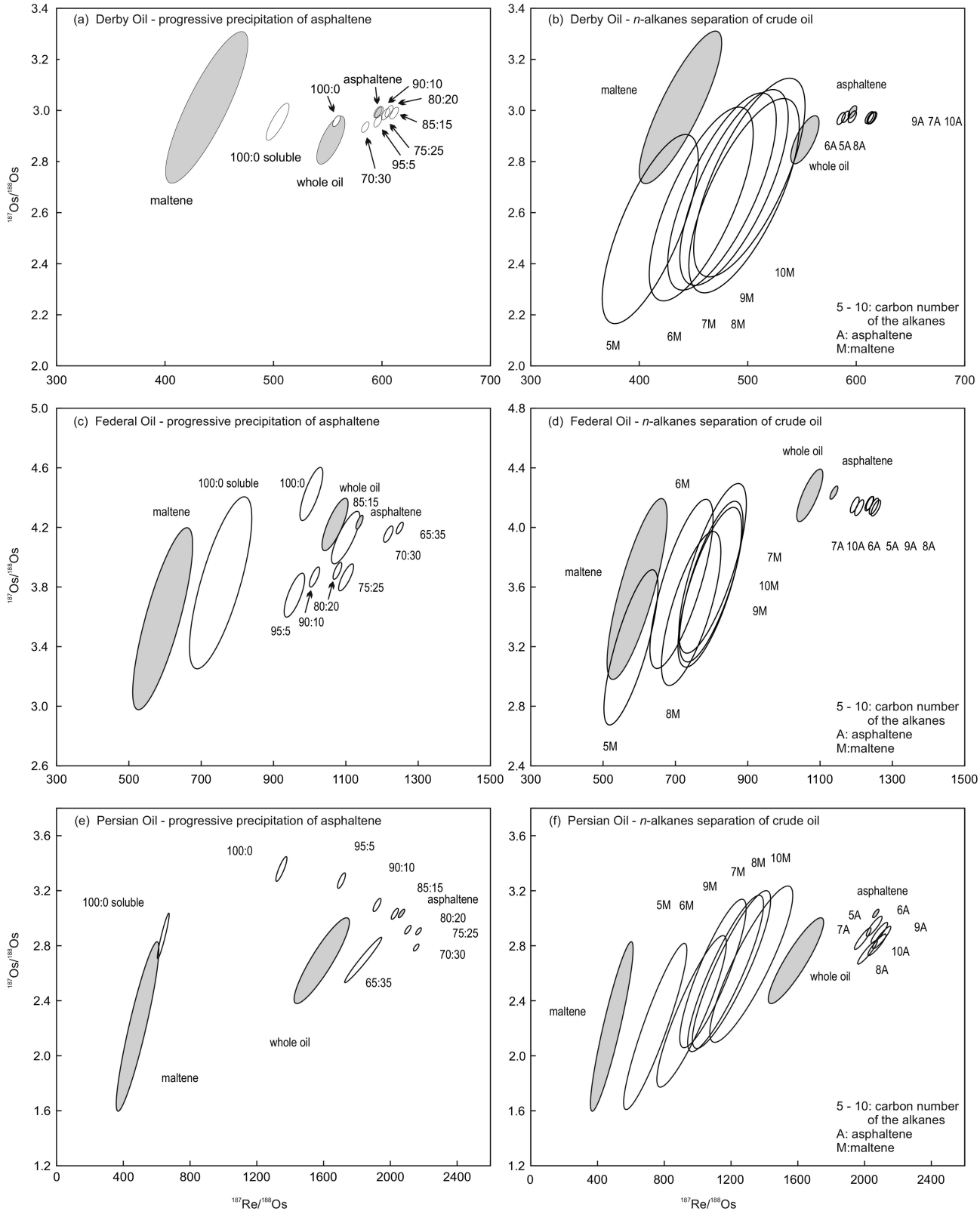
(a) Derby Oil - progressive precipitation of asphaltene
100:0
asphaltene
90:10
80:20
85:15
75:25
95:5
70:30
100:0 soluble
whole oil
maltene
(b) Derby Oil - n-alkanes separation of crude oil
maltene
asphaltene
9A 7A 10A
6A 5A 8A
whole oil
10M
9M
7M 8M
6M
5M
5 - 10: carbon number of the alkanes
A: asphaltene
M:maltene
(c) Federal Oil - progressive precipitation of asphaltene
100:0 soluble
100:0
whole oil
85:15
asphaltene
65:35
70:30
75:25
80:20
90:10
95:5
maltene
(d) Federal Oil - n-alkanes separation of crude oil
whole oil
asphaltene
6M
7A 10A 6A 5A 9A 8A
7M
10M
9M
maltene
8M
5M
5 - 10: carbon number of the alkanes
A: asphaltene
M:maltene
(e) Persian Oil - progressive precipitation of asphaltene
100:0
95:5
90:10
85:15
asphaltene
80:20
75:25
70:30
65:35
100:0 soluble
whole oil
maltene
(f) Persian Oil - n-alkanes separation of crude oil
10M
8M
7M
9M
5M 6M
asphaltene
5A
6A
7A
9A
10A
8A
whole oil
maltene
5 - 10: carbon number of the alkanes
A: asphaltene
M:maltene
187Os/188Os
187Re/188Os

Figure 9

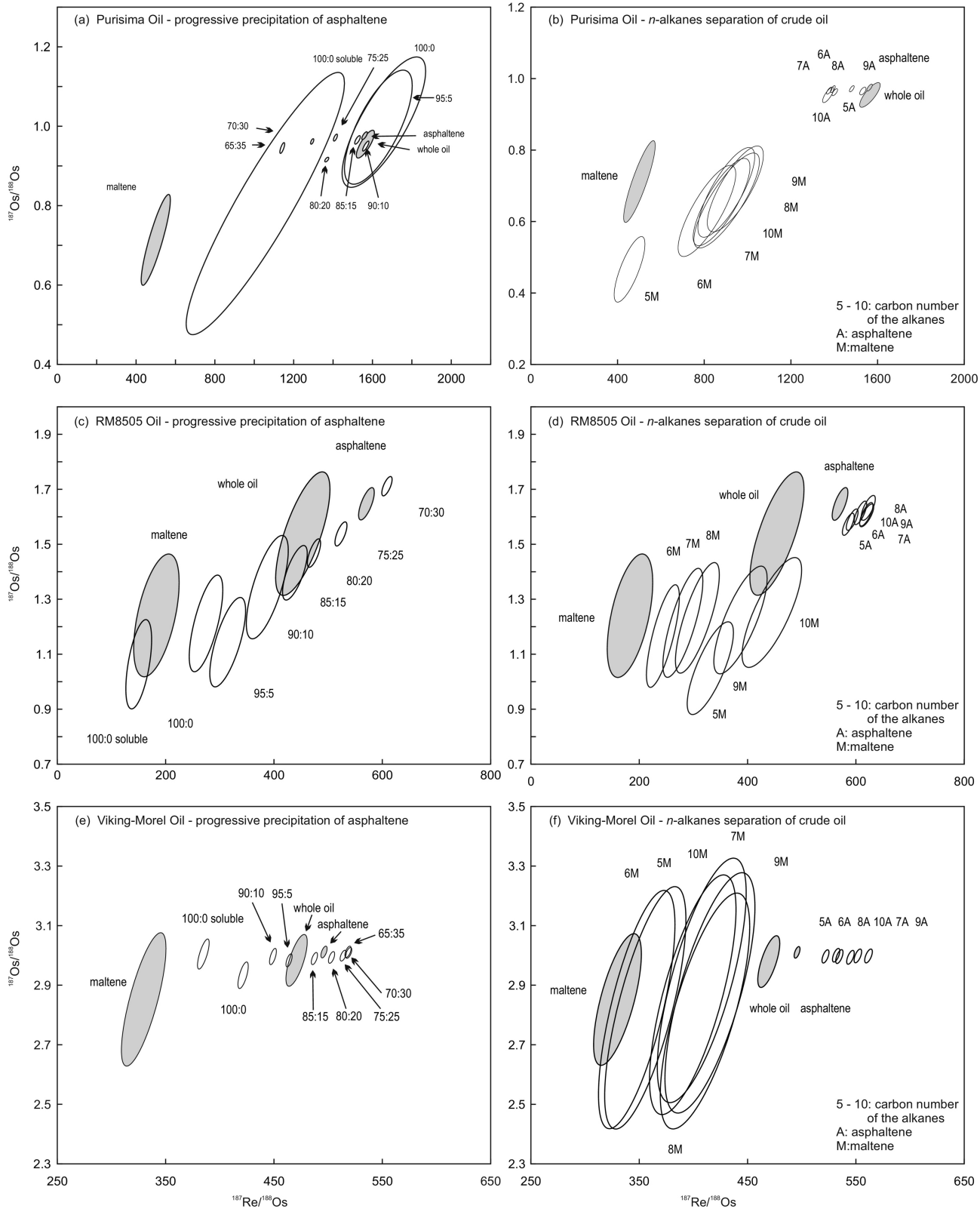
(a) Purisima Oil - progressive precipitation of asphaltene
100:0 soluble
75:25
100:0
95:5
70:30
65:35
asphaltene
whole oil
maltene
80:20
85:15
90:10
(b) Purisima Oil - n-alkanes separation of crude oil
6A
7A
8A
9A
asphaltene
whole oil
5A
10A
maltene
9M
8M
10M
7M
6M
5M
5 - 10: carbon number of the alkanes
A: asphaltene
M:maltene
(c) RM8505 Oil - progressive precipitation of asphaltene
asphaltene
whole oil
maltene
70:30
75:25
80:20
85:15
90:10
95:5
100:0
100:0 soluble
(d) RM8505 Oil - n-alkanes separation of crude oil
asphaltene
whole oil
8A
10A
9A
6A
7A
5A
6M
7M
8M
maltene
10M
9M
5M
5 - 10: carbon number of the alkanes
A: asphaltene
M:maltene
(e) Viking-Morel Oil - progressive precipitation of asphaltene
90:10
95:5
whole oil
100:0 soluble
asphaltene
65:35
maltene
70:30
100:0
85:15
80:20
75:25
(f) Viking-Morel Oil - n-alkanes separation of crude oil
7M
6M
5M
10M
9M
5A
6A
8A
10A
7A
9A
maltene
whole oil
asphaltene
8M
5 - 10: carbon number of the alkanes
A: asphaltene
M:maltene
187Os/188Os
187Re/188Os

Figure 10